



**EFFECT ON MAPE COMPATIBILIZER ON MECHANICAL
PROPERTIES OF WOOD FIBRE REINFORCED RECYCLED
POLYPROPYLENE COMPOSITE**



**BACHELOR OF MANUFACTURING ENGINEERING
TECHNOLOGY WITH HONOURS**

2024



**Faculty of Industrial and Manufacturing Technology and
Engineering**

**Effects on MAPE Compatibilizer on Mechanical Properties of Wood Fibre reinforced
Recycled Polypropylene Composites**

اونيورسيتي تيكنيكل مليسيا ملاك
UNIVERSITI TEKNIKAL MALAYSIA MELAKA

Ahmad Husaini Bi Nasardin

Bachelor of Manufacturing Engineering Technology with Honours

2024

**Effects on MAPE Compatibilizer on Mechanical Properties of Wood Fibre reinforced
Recycled Polypropylene Composites**

AHMAD HUSAINI BIN NASARDIN

**A thesis submitted
in fulfillment of the requirements for the degree of
Bachelor of Manufacturing Engineering Technology (BMMW) with Honours**



Faculty of Industrial and Manufacturing Technology and Engineering

UNIVERSITI TEKNIKAL MALAYSIA MELAKA

2024

BORANG PENGESAHAN STATUS LAPORAN PROJEK SARJANA

TAJUK: Effects on MAPE Compatibilizer on Mechanical Properties of Wood Fibre reinforced Recycled Polypropylene Composites

SESI PENGAJIAN: 2023/24 Semester 1

Saya **AHMAD HUSAINI BIN NASARDIN**

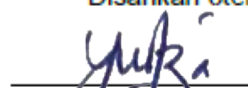
mengaku membenarkan tesis ini disimpan di Perpustakaan Universiti Teknikal Malaysia Melaka (UTeM) dengan syarat-syarat kegunaan seperti berikut:

1. Tesis adalah hak milik Universiti Teknikal Malaysia Melaka dan penulis.
2. Perpustakaan Universiti Teknikal Malaysia Melaka dibenarkan membuat salinan untuk tujuan pengajian sahaja dengan izin penulis.
3. Perpustakaan dibenarkan membuat salinan tesis ini sebagai bahan pertukaran antara institusi pengajian tinggi.
4. ****Sila tandakan (✓)**

- SULIT** (Mengandungi maklumat yang berdarjah keselamatan atau kepentingan Malaysia sebagaimana yang termaktub dalam AKTA RAHSIA RASMI 1972)
- TERHAD** (Mengandungi maklumat TERHAD yang telah ditentukan oleh organisasi/badan di mana penyelidikan dijalankan)
- TIDAK TERHAD**

Disahkan oleh:





Cop Rasmi:

TS. DR. YUSLIZA BINTI YUSUF
Pensyarah Kanan
Jabatan Teknologi Kejuruteraan Pembuatan
Fakulti Teknologi dan Kejuruteraan
Industri dan Pembuatan
Universiti Teknikal Malaysia Melaka

Tarikh: 8 JANUARY 2024

Tarikh: 7/2/2024

****** Jika tesis ini SULIT atau TERHAD, sila lampirkan surat daripada pihak berkuasa/organisasi berkenaan dengan menyatakan sekali sebab dan tempoh laporan PSM ini perlu dikelaskan sebagai SULIT atau TERHAD.

DECLARATION

I declare that this Choose an item. entitled “Effects on MAPE Compatibilizer on Mechanical Properties of Wood Fibre reinforced Recycled Polypropylene Composites” is the result of my own research except as cited in the references. The Choose an item. has not been accepted for any degree and is not concurrently submitted in candidature of any other degree.

Signature

:



Name

:

Ahmad Husaini Bin Nasardin

Date

:

8 JANUARY 2024



APPROVAL

I hereby declare that I have checked this thesis and in my opinion, this thesis is adequate in terms of scope and quality for the award of the Bachelor of Manufacturing Engineering Technology (BMMW) with Honours.

Signature : 
Supervisor Name : Ts. Dr. Yusliza Binti Yusuf
Date : 7/2/2024



DEDICATION

This study is especially dedicated to my wonderful parents, who have always provided the moral, spiritual, emotional, and material support that I deserved when I considered giving up.

Not to mention my sibling, sister and brother, family, academic adviser, and supervisor Ts. Dr. Yusliza binti Yusof, friends, and classmates who gave me guidance and motivation to complete this study.

Last but not least, I dedicate this book to The Almighty "Allah," thanking you for your guidance, strength, mental power, protection, abilities, and gift of life.

اونيورسيتي تيكنيكل مليسيا ملاك

UNIVERSITI TEKNIKAL MALAYSIA MELAKA

ABSTRACT

The main goal of this research is to investigate the ways in which the mechanical and physical properties of filament and filament were affected by varying loadings of maleic anhydride grafted polyethylene (MAPE). This research project involved the production of 3D printing filament using a material composed of recycled polypropylene/wood fibre (r-WoPPc) and MAPE. Additionally, the mechanical properties of a sample of 3D printer filament formed of r-WoPPc and the addition of MAPE were evaluated. After being supplied in small bits, wood fibre (WF) would go through a number of operations before being sieved to a size of 125 microns. An alkaline treatment with a solution of sodium hydroxide (NaOH) at a concentration of 6% was effective in treating wood flies. For the purpose of enhancing the tensile characteristics of WF, NaOH was utilised. At a temperature of 80 degrees Celsius and for a period of twenty-four hours, the WF was brought into the oven for treatment. For the purpose of producing a composite that is both robust and long-lasting, with particular mechanical qualities, the hot press method of mixing PP with treated WF and the addition of MAPE loading percentage was utilised. Once the composite has been allowed to cool, it will next be subjected to a crushing process in order to be transformed into pellet form. Fabrication of 3D printing filaments utilising a single extruder by inserting varying levels of MAPE loading (0%, 1%, 3%, and 5%) into a WF and PP as matrix as reinforcement in order to determine the mechanical and physical properties of the filaments as well as their surroundings, such as water absorption. To make the filament, the extrusion process will be aided by a single extruder machine, and the temperature setting parameter will be set to 180 degrees Celsius. Both the rod specimen (ASTM D790) and the dog bone specimen (ASTM D638) are being manufactured in three sets for each percentage of MAPE loading. A loading of 1% of MAPE into r-WoPPc is considered to be the best MAPE loading for the anticipated outcome of this experiment. Due to the increased wettability and plasticization of the WF, the incorporation of 1 weight percent of MAPE prior to the installation of MAPE improved the interfacial contacts between the WF and the matrix and protected the WF from having its integrity compromised during the reprocessing process. When compared to the 0wt% MAPE, the 1wt% MAPE yields a result that is significantly different. According to the percentage of MAPE loading, the increase in the result of mechanical characteristics and physical properties is referred to as the increment. On the other hand, the selection of 1 weight percent MAPE was the source of the significant result on the tests because the rise in the result from 1 weight percent MAPE to 5 weight percent is just slight. When the MAPE content was increased from 1 to 5 weight percent, there was also an increase in the number of big WFs.

ABSTRAK

Matlamat utama penyelidikan ini ialah untuk menyiasat cara-cara di mana sifat mekanikal dan fizikal filament dan filament dipengaruhi oleh beban yang berbeza daripada maleic anhydride grafted polyethylene (MAPE). Projek penyelidikan ini melibatkan pengeluaran 3D printing filament menggunakan bahan yang terdiri daripada polipropilena/gentian kayu kitar semula (r-WoPPc) dan MAPE. Selain itu, sifat-sifat mekanikal sampel 3D printer filament terbentuk daripada r-WoPPc dan penambahan MAPE telah dinilai. Selepas dibekalkan dalam bit kecil,

gentian kayu (WF) akan melalui beberapa operasi sebelum ditutup kepada saiz 125 mikron. Rawatan alkali dengan larutan natrium hidroksida (NaOH) pada kepekatan 6% berkesan dalam merawat lalat kayu. Untuk tujuan meningkatkan ciri-ciri tegangan WF, NaOH digunakan. Pada suhu 80 darjah Celsius dan untuk tempoh dua puluh empat jam, WF dibawa ke dalam oven untuk rawatan. Untuk tujuan menghasilkan komposit yang kuat dan tahan lama, dengan kualiti mekanikal tertentu, kaedah pers panas campuran PP dengan WF dirawat dan penambahan peratusan beban MAPE digunakan. Sebaik sahaja komposit telah dibenarkan untuk sejuk, ia akan diikuti dengan proses memecah untuk diubah menjadi bentuk pelet. Pembuatan filamen percetakan 3D menggunakan ekstruder tunggal dengan memasukkan tahap yang berbeza beban MAPE (0%, 1%, 3%, dan 5%) ke dalam WF dan PP sebagai matriks sebagai penguatkuasaan untuk menentukan sifat mekanikal dan fizikal filamen serta persekitaran mereka, seperti penyerapan air. Untuk membuat filamen, proses ekstrusi akan dibantu oleh mesin ekstruder tunggal, dan parameter tetapan suhu akan ditetapkan kepada 180 darjah Celsius. Kedua-dua sampel batang (ASTM D790) dan sampel tulang anjing (ASTM D638) sedang dihasilkan dalam tiga set untuk setiap peratusan beban MAPE. Satu muat 1% daripada MAPE ke r-WoPPc dianggap sebagai muat terbaik untuk hasil yang dijangka daripada eksperimen ini. Kerana peningkatan kelembapan dan plasticization WF, penyertaan 1 peratus berat MAPE sebelum pemasangan MAPE meningkatkan hubungan antara WF dan matriks dan melindungi WF daripada mempunyai integriti terjejas semasa proses pemprosesan semula. Apabila dibandingkan dengan 0wt% MAPE, 1wt% mAPE menghasilkan hasil yang sangat berbeza. Mengikut peratusan muatan MAPE, peningkatan hasil ciri-ciri mekanikal dan sifat fizikal dikenali sebagai peningkatan. Di sisi lain, pemilihan 1 peratus berat MAPE adalah sumber hasil yang signifikan pada ujian kerana peningkatan dalam hasil daripada 1 peratusan berat mAPE kepada 5 peratus besar hanya sedikit. Apabila kandungan MAPE meningkat daripada 1 kepada 5 peratus berat, terdapat juga peningkatan dalam bilangan WF besar.

ACKNOWLEDGEMENTS

In the Name of Allah, the Most Gracious, the Most Merciful

First and foremost, I want to thank and honor Allah the Almighty, my Creator and Sustainer, for everything I have received since the beginning of my life. I would like to thank Universiti Teknikal Malaysia Melaka (UTeM) for providing the study platform.

My heartfelt gratitude goes to my supervisor, Ts. Dr. Yusliza binti Yusof of Universiti Teknikal Malaysia Melaka (UTeM), for her unwavering encouragement, counsel, and inspiration. Her unwavering patience in mentoring and imparting invaluable insights will be remembered forever. Also, thank you to my group member Nurul Asyikin binti Omar for always being there for me on my journey. I would also like to thank all my course mates for providing me with a wealth of information and encouragement.

Finally, I want to express my heartfelt thanks to my dear mother, Raja Aminah Binti Raja Lop, who has been a pillar of support in all my endeavours. and, my siblings, who are constantly morally and financially supportive, as well as praying for me. Finally, I'd like to express my gratitude to everyone who helped, supported, and inspired me to begin my studies.



TABLE OF CONTENTS

	PAGE
DECLARATION	
APPROVAL	
DEDICATION	
ABSTRACT	i
ABSTRAK	ii
ACKNOWLEDGEMENTS	iii
TABLE OF CONTENTS	iv
LIST OF TABLES	vi
LIST OF FIGURES	vii
LIST OF SYMBOLS AND ABBREVIATIONS	x
LIST OF APPENDICES	xi
CHAPTER 1 INTRODUCTION	12
1.1 Background	12
1.2 Problem Statement	14
1.3 Research Objective	15
1.4 Scope of Research	16
CHAPTER 2 LITERATURE REVIEW	17
2.1 Introduction	17
2.2 3D Printing Technology	18
2.2.1 Types of 3D Printing Technology	19
2.2.2 3D Printing Technology Application	27
2.2.3 3D printing Filament Material	30
2.3 Polypropylene as Matrix in Composite	31
2.3.1 Recycled Polypropylene	32
2.3.2 Recycled Polypropylene Properties and Application	33
2.4 Wood Fiber as Reinforced Material in Composite	34
2.4.1 Wood Fibre Physical and Mechanical Properties	34
2.4.2 Example of Wood Fiber Application as Reinforced Materials	38
2.5 Maleated Anhydride Polyethylene Coupling Agent	41
2.6 Summary of Literature Review	42
CHAPTER 3 METHODOLOGY	43
3.1 Introduction	43

3.2	Preparation of Material	45
3.2.1	Recycled Polypropylene (rPP)	45
3.2.2	Wood Dust	46
3.2.3	NaOH Solution	51
3.2.4	Preparation of MAPE	56
3.3	Fabrication of Filament	57
3.3.1	Preparation of Recycled Polypropylene/Wood Dust/MAPE Composite	57
3.3.2	Hotpress Process	58
3.3.3	Crusher Process	63
3.3.4	Extrusion Process	66
3.4	3D Printing Process	68
3.5	Physical Properties (Water Absorbtion)	70
3.6	Mechanical Test	72
3.6.1	Mechanical (Tensile)	72
3.6.2	Mechanical (Flexural)	74
CHAPTER 4 RESULTS AND DISCUSSION		77
4.1	Introduction	77
4.2	3D Printing Filament Produced	77
4.2.1	Extrusion	77
4.3	3D Printing Sample	81
4.3.1	3D Printing	81
4.4	Physical Properties	83
4.4.1	Water Absorption	83
4.5	Mechanical Properties	85
4.5.1	Tensile Test	85
4.5.2	Flexural Test	92
4.6	Summary	99
CHAPTER 5		101
5.1	Conclusion	101
5.2	Recommendations	103
5.3	Project Potential	104
REFERENCES		105
APPENDICES		109

LIST OF TABLES

TABLE	TITLE	PAGE
Table 2.1	Classification of different AM processes based on the ASTM standards.	20
Table 2.2	Selected characteristic values for soft- and hardwood according to EN 338(Olsson et al., 2013)	36
Table 2.3	comprises both tensile and bending data	38
Table 3.1	Step in Sieving process	48
Table 3.2	Specification of Sodium Hydroxide	51
Table 3.3	Weight Ratio of Water	52
Table 3.4	The amount of wood dust fibre, recycled polypropylene (PP), and MAPE	57
Table 3.5	Hotpress process	59
Table 3.6	Crush Process	64
Table 3.7	The filament extrusion processing parameters.	68
Table 3.8	Printing settings	70
Table 3.9	Procedure Tensile Test	73
Table 3.10	Procedure Flexural Test	75
Table 4.1	Result of the water absorption for R-WoPPc with different loading MAPE	84
Table 4.2	The average Tensile Strength and Modulus Elasticity	91
Table 4.3	The average Flexural Strength and Elasticity	97

LIST OF FIGURES

FIGURE	TITLE	PAGE
Figure 2.1	Binder jetting (K Srinivasulu & Solomon Dufera, 2019)	21
Figure 2.2	Directed energy deposition.	22
Figure 2.3	Material extrusion	23
Figure 2.4	Material jetting (Gülcan et al., 2021)	24
Figure 2.5	Powder bed fusion(K Srinivasulu Reddy & Solomon Dufera Tolcha, 2019)	25
Figure 2.6	Sheet lamination	26
Figure 2.7	Vat photopolymerization(K Srinivasulu Reddy & Solomon Dufera Tolcha, 2019)	27
Figure 2.8	Polypropylene's atomic chain.	31
Figure 2.9	Structure of cellulose(Ndibewu & Tchieta, 2018)	34
Figure 2.10	Structure of hemicellulose(Ndibewu & Tchieta, 2018)	35
Figure 2.11	Structure of Lignin(Muktham et al., 2016)	36
Figure 2.12	Microscopic structure of densified wood (a) and comparison of the variability of tensile strength (b) and modulus of elasticity (c) of normal and densified wood, respectively(Jakob et al., 2022)	38
Figure 2.13	Polyethylene-graft-maleic anhydride (PE)	42
Figure 3.1	The flow of the research methodology.	44
Figure 3.2	the raw material of recycled polypropylene.	45
Figure 3.3	show the raw material of the wood	46
Figure 3.4	Sieving Machine	47

Figure 3.5 NaOH on Liquid Form	51
Figure 3.6 NaOH Solution	52
Figure 3.7 NaOH Treatment	54
Figure 3.8 Cleaning Wood Fibre using Distilled Water	55
Figure 3.9 The Drying Process	56
Figure 3.10 shows the maleated anyhydride grafted polyethylene (MAPE)	56
Figure 3.11 Hotpress Machine	59
Figure 3.12 the type of crusher machine.	64
Figure 3.13 Single extruder machine	66
Figure 3.14 cooling water bath	67
Figure 3.15 filament traction rollers	67
Figure 3.16 FDM 3D printing	69
Figure 3.17 Type of specimen	69
Figure 3.18 Equation of Water Absorption	71
Figure 3.19 Oven used to Dried Specimen	72
Figure 3.20 Tensile test Machine	73
Figure 3.21 Flexural Test Machine	75
Figure 4.1 Entry hole of Cooling Bath	78
Figure 4.2 Sample filament sticky at entry hole cooling bath	79
Figure 4.3 Printing Filament	79
Figure 4.4 Filament & Microscope image of 0% MAPE	80
Figure 4.5 Filament & Microscope image of 1% MAPE	80
Figure 4.6 Filament & Microscope image of 3% MAPE	80
Figure 4.7 Filament & Microscope image of 5% MAPE	81

Figure 4.8 Specimen Bent	82
Figure 4.9 Type of Specimen	83
Figure 4.10 Water Absorption for 24 Hours	85
Figure 4.11 Tensile Strength of 0% MAPE loading	86
Figure 4.12 Tensile Strength of 1% MAPE loading	87
Figure 4.13 Tensile Strength of 3% MAPE loading	88
Figure 4.14 Tensile Strength of 5% MAPE loading	89
Figure 4.15 Tensile Strength of r-WoPPc	91
Figure 4.16 Modulus Elasticity of r-WoPPc	92
Figure 4.17 Flexural Strength of 0% MAPE loading	93
Figure 4.18 Flexural Strength of 1% MAPE loading	94
Figure 4.19 Flexural Strength of 3% MAPE loading	95
Figure 4.20 Flexural Strength of 5% MAPE loading	96
Figure 4.21 Flexural Strength of r-WoPPc	98
Figure 4.22 Elasticity of r-WoPPc	99

LIST OF SYMBOLS AND ABBREVIATIONS

D,d	-	Diameter
cm	-	Centimeter
mm	-	Millimeter
Mpa	-	Mega Pascal
%	-	Percent
wt.	-	weight
kN	-	Kilo Newton
Kg	-	Kilogram
g	-	Gram
°	-	Degree
µm	-	Micrometer
rPP	-	Recycled polypropylene
WPC	-	Wood plastic composite
UH	-	Ultra High
PP	-	Polypropylene
NaOH	-	Sodium Hydroxide
WD	-	Wood Dust
MAPE	-	Maleated Anhydride Grafted Polyethylene
WF	-	Wood Fibre
r-WoPPc	-	Recycled Wood fibre/Polypropylene
WAR	-	Water Absorption Rate

LIST OF APPENDICES

APPENDIX	TITLE	PAGE
APPENDIX A	Gantt Chart for PSM1	109
APPENDIX B	Gantt Chart for PSM2	110



CHAPTER 1

INTRODUCTION

1.1 Background

Additive manufacturing, or 3D printing, has experienced significant advancements in the past decade. It offers advantages such as the ability to create complex shapes and customized products without specialized tools. Fused Deposition Modeling (FDM) is a popular 3D printing technique that melts filament layer by layer to build objects. Bio-composite filaments, derived from renewable sources, have emerged as an appealing alternative to synthetic filaments. They offer affordability, strength, and environmental sustainability. By utilizing bio-composite filaments, 3D printing can contribute to reducing reliance on traditional plastics and drive advancements in manufacturing technologies (Saad et al., 2022). Interest in biodegradable 3D printing has grown with the development of environmentally friendly materials like wood, cellulose, sugars, and lignin. Wood particle-based composites have entered the market, and various 3D printing techniques, including FDM, injection powder printing, and liquid/paste deposition modeling, are being used for printing with wood. These advancements offer sustainable options and utilize renewable resources in manufacturing processes (Shahrubudin et al., 2019).

Natural fibers are gaining popularity as reinforcing agents in polymeric composites due to their technological, environmental, and economic benefits. They are being recognized as a viable alternative to synthetic fibers because of their diversity, availability, and renewability. However, the bonding strength between wood fibers (a polar-hydrophilic material) and polyolefins (non-polar-hydrophobic polymers) is insufficient. To address this, a

compatibilizer or coupling agent needs to be added to enhance the bonding strength between the wood fibers and the polymer matrix. Significant efforts have been made to improve the interface between wood fibers and polymers. One effective coupling agent for Wood Polymer Composites (WPC) is maleic anhydride-grafted polymer (Rahayu et al., 2020).

This study utilized MAPE as a coupling agent to investigate the role of esterification in the interfacial adhesion of wood fiber polyethylene composites. UH-WPCs were successfully extruded using HDPE or MAPE as the polymer matrix with varying wood fiber percentages. The mechanical properties, creep behavior, water absorption, and surface contact angle of UH-WPCs were analyzed with and without MAPE. The study also explored the interfacial adhesion mechanism using polymer matrix blends and separated wood fibers (Zhou et al., 2022). To enhance the strength of the composite, various studies have explored the use of maleated polyolefins (MAPE and MAPP) as coupling agents in wood-plastic composites (WPCs). Adding 1% to 5% MAPE or MAPP to the mix can improve the mechanical characteristics of the composite (r-WoPPc). In a specific investigation, maleated polyethylene (MAPE) was examined as a coupling agent in recycled polypropylene (PP) and wood dust fiber (WDF). MAPE was added during the mixing step, and its influence on the compatibility of the (r-WoPPc) composite was studied.

1.2 Problem Statement

The remarkable progress in the development of biofiber composites over the past few decades has been truly fascinating. Through extensive research into innovative compositions and techniques, these materials have now reached a level of performance that is truly impressive. This ongoing exploration has led to their successful development and widespread implementation, making them an intriguing field of study (Faruk et al., 2012). The recycling of wood-plastic composites (WPCs) poses challenges as their mechanical, physical, and thermal properties are noticeably compromised with each recycling cycle. However, there is potential for mitigating this issue through the reprocessing of waste industrial WPCs. By combining virgin WPCs with waste materials in specific ratios, it is possible to preserve the mechanical qualities of the WPCs to some extent even after undergoing multiple recycling cycles. This approach offers a promising solution to maintain the performance of recycled WPCs (Zhou et al., 2022).

Insufficient stress transmission between the polymer matrix and wood fibers due to weak interfacial adhesion is a common issue in wood-plastic composites (WPCs), leading to a decline in their mechanical properties. To address this challenge, several studies have focused on improving the compatibility of the two components. This involves enhancing the wettability of the polymer matrix and the dispersibility of the wood fibers. By achieving better compatibility, the interfacial adhesion can be strengthened, resulting in improved mechanical properties of WPCs (Hao et al., 2021). Maleated polyolefins (MAPE) have emerged as widely utilized and effective coupling agents in addressing the issue of weak interfacial adhesion in wood-plastic composites (WPCs). These coupling agents play a crucial role in improving the compatibility between the hydrophobic polyolefin matrix and hydrophilic wood fibers. MAPE contain reactive functional groups that can react with both

14 the polymer matrix and wood fibers, leading to enhanced interfacial bonding. This results

in improved stress transfer, increased interfacial adhesion, and enhanced mechanical properties of the WPCs. The addition of MAPE to WPC formulations has been shown to significantly enhance the wettability of the polymer matrix and the dispersibility of the wood fibers, ultimately improving the overall performance and durability of WPC materials (Lu et al., 2005). This issue can be remedied by using maleated polyofins. It is possible to provide a 30- 100% improvement in the mechanical properties of WPCs by adding 1-5 weight percent of MAPE (Hao et al., 2021a).

This research project aims to develop a 3D printing filament material that uses MAPE as a coupling agent and wood fibre reinforced recycled polypropylene composites. Finding a solution to an environmental issue and developing biodegradable polymer are the goals of this study. Ascertaining the impact of MAPE on the morphology and tensile strength of the composite material's mechanical characteristics is the second step.

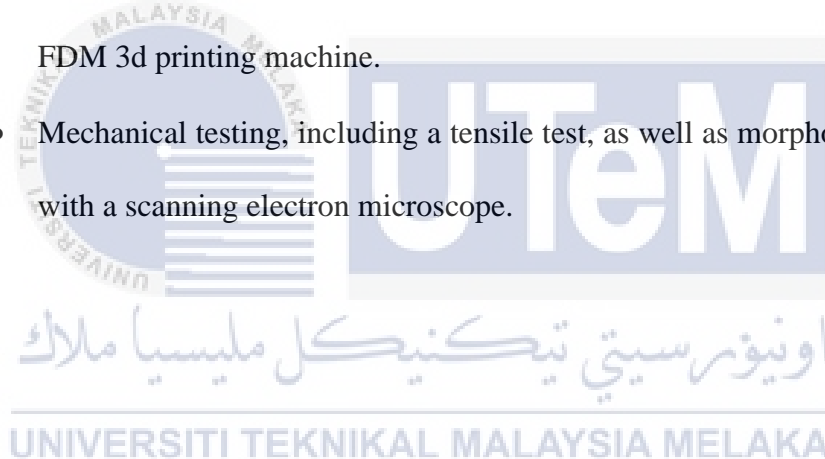
1.3 Research Objective

The aim of this research is to study the physical, mechanical, and morphological properties of recycle polypropylene (PP) and recycle wood dust as reinforcement natural fiber by adding maleated-anhydride-grafted polyethylene (MAPE). Specifically, the objective as follows:

- a) To fabricate a new 3D printer filament from recycle Polypropylene (PP), wood fiber and maleic anhydride polyethylene (MAPE).
- b) To Evaluate the effect of maleic anhydride polyethylene (MAPE) on the mechanical properties of the composite material, including tensile strength, flexural strength and water absorption.

1.4 Scope of Research

- The preparation of wood fiber required the use of a sieve as well as polypropylene.
- The proportion of wood fiber to polypropylene that is present in the material before it is mixed
- Determine the percentage of maleic anhydride polyethylene (MAPE) that has to combine with the wood fiber and the polypropylene.
- The use of machine such as an extrusion machine, a hot press, a crusher and FDM 3d printing machine.
- Mechanical testing, including a tensile test, as well as morphological testing with a scanning electron microscope.



CHAPTER 2

LITERATURE REVIEW

2.1 Introduction

In the industry, the words "plastic" and "polymer" are frequently used interchangeably. Polymers, which can be formed by joining chains of molecules, are plastics. Plastics may be made into nearly any form, sheet, or foam by moulding, stretching, casting, or blasting them. They can even be made into textile threads. The practice of additive manufacturing (AM), also referred to as 3D printing, has gained popularity throughout time, and new developments are frequently launched. 3D printing is the process of layering materials to create three-dimensional objects. Pure polymers, polymer matrix composites, polymer ceramic composites, nanocomposites, and fiber-reinforced composites are just a few of the materials that have been used in the AM process. Each of these materials has distinct qualities and important elements including material kind, texture, cost, and so on. Plastic waste made from petroleum, however, is expensive and challenging to recycle. To solve this issue, a biodegradable product made from renewable resources, such as recycled polypropylene, should be developed. Today, the section opens with an introduction to the science behind 3D printing and a list of the main plastics used to make filament for 3D printers. It will then discuss the natural fiber and composite materials that are now available for 3D printing. The second step is to look at some relevant information on the materials being considered for this work, which is a maleic anhydride grafted polyethylene (MAPE) coupling agent for natural fibers with a focus on recycled PP (Polypropylene). Additionally,

a thorough examination of the manufacturing process used to create the filament as well as some theoretical details on the other method employed in the experiment were provided.

2.2 3D Printing Technology

A synonym for 3D printing is additive manufacturing. Additive manufacturing was employed for prototyping at the beginning of the 1980s, but due to its accuracy, reproducibility, and affordable production costs, it has recently gained favor (Shaik et al., 2021). Depending on the use, there are several types of 3D printing. Several examples include SLA (Stereolithography), FDM/FFF (Fused Deposition Modeling/Fused Filament Fabrication), Material Extrusion, Binder Jetting, Powder Jetting, and Direct Energy Deposition. For creating prototypes and custom thermoplastic parts, some of the most effective 3D printing processes are available (Shaik et al., 2021). Since Charles Hull's conception of a stereolithography-based computer system that reads data from a CAD file using the STL file format in 1984, various uncommon sorts of 3D printers have been put into practice. The STL file contains details about the printed object's color, texture, and thickness, among other things. Many printing devices have been created to print a variety of things on different scales in a variety of industries (such the food and automobile) (Shahrubudin et al., 2020). According to J. Y. Lee et al., 2017 the use of 3D printing has become more widespread and effective in the field of advanced manufacturing. Many nations have embraced this technology, especially those with robust manufacturing sectors.

Globally, additive manufacturing is becoming more and more popular, notably in the healthcare, biomedical, aerospace, and building sectors (Shahrubudin et al., 2020). A relatively new technology that is continually changing is 3D printing. It is being used in health education after experiencing tremendous growth. A new generation of surgeons could become more knowledgeable and skilled with the help of patient-specific models created

from imaging datasets with anatomical integrity (Garcia et al., 2018). The government and local practitioners in Malaysia have been asked to encourage the development of this technology for a range of sectors, particularly biomedical products, as a result of the lack of adoption of this technology by local businesses. The goal of the current study is to describe the problems encountered by biomedical industries that use 3D printing technology in their production processes. Qualitative approaches, particularly in-depth interviews, were used to investigate the challenges faced by manufacturing companies while designing 3D printed biomedical items (Shahrubudin et al., 2020). In conclusion, 3D printing technology has developed recently into a flexible and effective tool in the advanced manufacturing industry. Many countries use this method extensively, especially in the industrial sector. As a result, this article offers a summary of the various 3D printing processes, their uses, and, finally, the materials that are used in the manufacturing industry (Shahrubudin et al., 2019).

2.2.1 Types of 3D Printing Technology

Technologies for 3D printing have been developed with a variety of uses. Binding jetting, directed energy deposition, material extrusion, material jetting, powder bed fusion, sheet lamination, and vat photopolymerization are the seven categories into which 3D printing techniques are divided in accordance with ASTM Standard F2792. Since each has a unique set of applications, there is no debate over which performs better: technology or machines. The use of 3D printing technology to make a variety of objects is quickly expanding beyond prototypes (Wang et al., 2017). Table 2.1 provides a classification of several AM techniques according to ASTM standards.

Table 2.1 Classification of different AM processes based on the ASTM standards.

Binder jetting	Direct energy deposition	Material extrusion	Material jetting	Powder bed fusion	Sheet lamination	Vat photopolymerization
Voxeljet	Laser Engineered Net Shaping (LENS)	Fused Deposition Modeling (FDM)	Stratasys' Polyjet	Selective Laser Sintering (SLS)	Laminated Object Manufacturing (LOM)	Stereolithography Apparatus (SLA)
ExOne			3D System's Multi-Jet Printing (MJM)	Selective Laser Melting (SLM)	MCor's A4 Paper Printing	Digital Light Processing (DLP)
Color Jet Printing (CJP)			Solidscape	Electron Beam Melting (EBM)	Kira' Paper Lamination Technology (PLT)	

There is the explanation of the types of 3D printing below:

I. Binder jetting

Binder jetting is a rapid prototyping and 3D printing method that combines powder particles by selectively depositing a liquid binding agent. The layer is created using the binder jetting technique by sprinkling a chemical binder over the dispersed powder. (Low et al., 2017). Casting patterns, unfinished sintered objects, or comparable large-volume things can be created from sand via binder jetting. Binder jetting can be used to print ceramics, sand, metals, polymers, and hybrids. Sand, for example, didn't need to be processed farther than other materials. Binder jetting is a straightforward, quick, and affordable procedure because powder particles are bonded together. Lastly, binder jetting has the

capacity to print large items (Shahrubudin et al., 2019). Figure 2.1 shown the example of binder jetting machine.

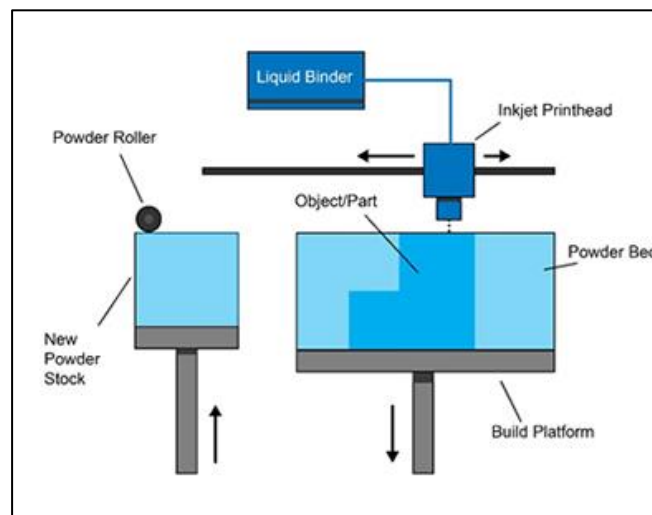


Figure 2.1 Binder jetting (K Srinivasulu & Solomon Dufera, 2019)

II. Directed energy deposition

The more difficult printing process known as directed energy deposition is frequently used to upgrade or add material to already existing components. The grain structure can be greatly controlled by directed energy deposition, which also produces high-quality products. Theoretically, directed energy deposition is like material extrusion, with the nozzle moving in multiple directions as opposed to being fixed to one axis. Metals and metal-based hybrids in the form of wire or powder are where the technology is most frequently used, although it can also be applied to ceramics and polymers. Laser deposition and laser engineered net shaping (LENS) are examples of this technology (Tofail et al., 2018). The creation or repair of objects with sizes ranging from millimeters to meters is now possible thanks to a brand-new technique called laser deposition. Laser deposition technology is gaining popularity in the manufacturing, transportation, aerospace, and oil and gas sectors due to its scalability and variety of capabilities in a single

system. In the meantime, during the casting process, laser LENS can employ heat energy to melt components (Dilberoglu et al., 2017). An example of a directed energy deposition setup is shown in Figure 2.2.

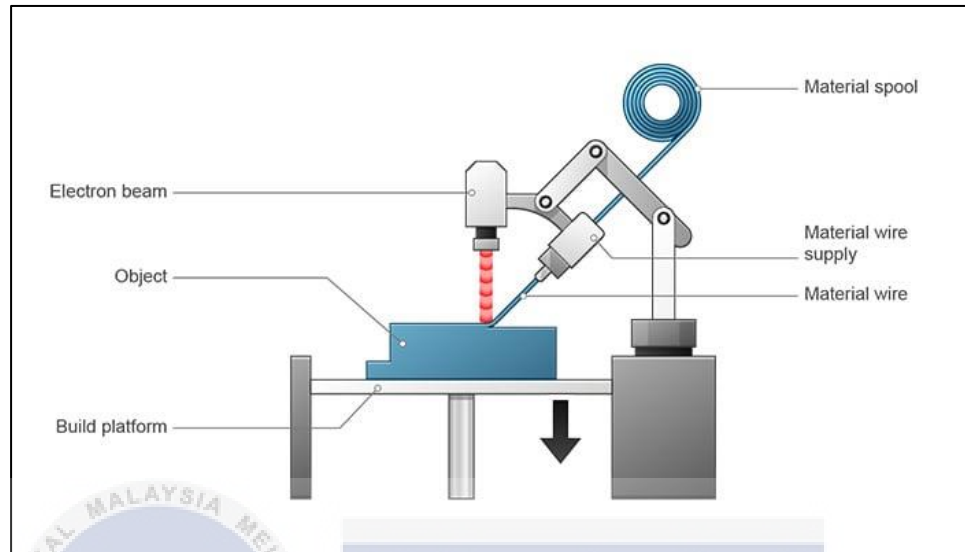


Figure 2.2 Directed energy deposition.

III. Materials extrusion

Material extrusion-based 3D printing can produce multi-material and multi-color polymers, food, and biological cells. This treatment has modest costs and is often utilized. Furthermore, this technology may provide completely functional product pieces (Tofail et al., 2018). The major material used in FDM, which was created in the early 1990s, is polymer. FDM generates components layer by layer by heating and extruding thermoplastic filament, depositing the filament in ultra-fine beads along the extrusion route and adding removable support materials where suitable, such as strong plastic for making 3D bone models (Yap et al., 2017). An example of the material extrusion setup is shown in Figure 2.3.

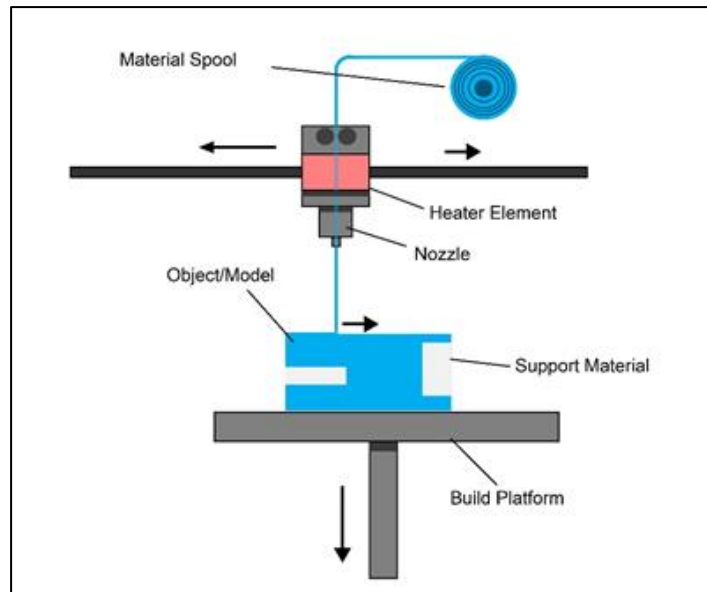


Figure 2.3 Material extrusion

IV. Material jetting

According to ASTM Standards, material jetting is a 3D printing process that involves drop-by-drop placement of construction material. A printer sprays droplets of a photosensitive substance that solidify and assemble components layer by layer under ultraviolet (UV) light in material jetting (Silbernagel, 2018). Material jetting, on the other hand, generates products with a highly smooth surface finish and high dimensional precision. Material jetting enables multi-material printing and the use of a diverse range of materials, including polymers, ceramics, composites, biologicals, and hybrids (Tofail et al., 2018). Figure 2.4 shows the material jetting setup.

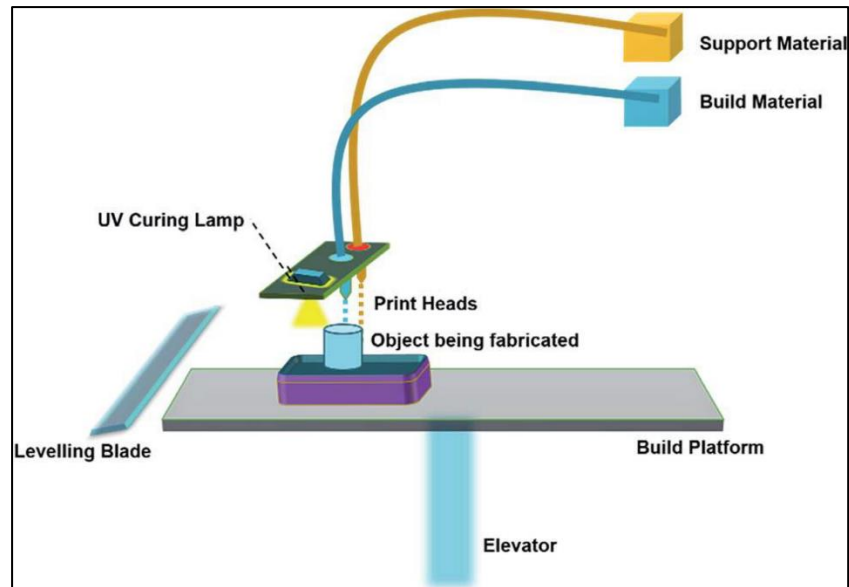


Figure 2.4 Material jetting (Gülcan et al., 2021)

V. Powder bed fusion

Powder bed fusion printing technologies include selective laser sintering (SLS), electron beam melting (EBM), and heat sintering (SHS). A laser or an electron beam is employed in this process to melt or fuse the material particles together. Metals, ceramics, polymers, composites, and hybrids are among the materials employed in this approach. The most well-known type of powder-based 3D printing is SLS, or selective laser sintering (Shahrubudin et al., 2019). Carl Deckard invented SLS technology in 1987. SLS is a 3D printing technology with variable surface polish that is functionally quick and accurate (Tiwari et al., 2015). Selective laser sintering can be used to create metal, plastic, and ceramic items. SLS created a three-dimensional object by sintering polymer particles with a powerful laser. While SHS technology, a subset of 3D printing technology, employs a head thermal print to melt thermoplastic material in order to generate a 3D printed item. The final improvement to an energy source for heating the

material comes from electron beam melting (Shahrubudin et al., 2019). The example of powder bed fusion setup is shown in Figure 2.5.

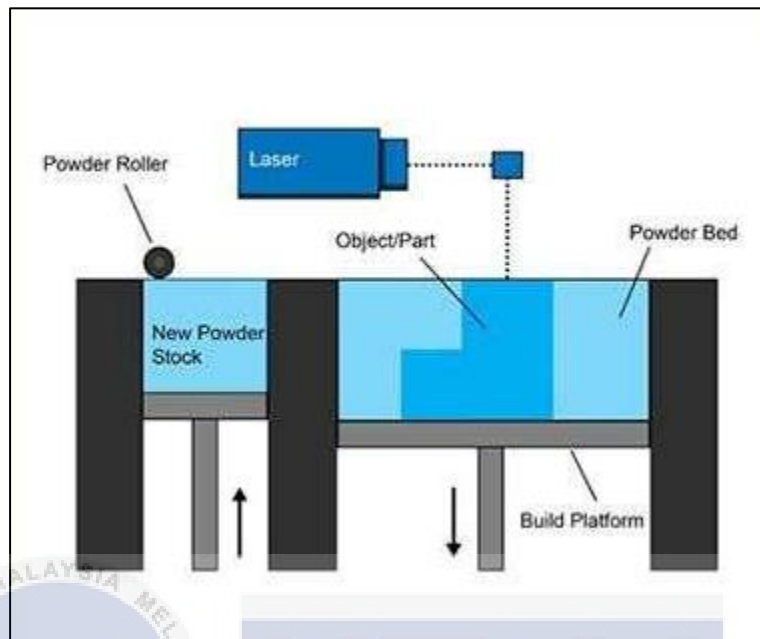


Figure 2.5 Powder bed fusion (K Srinivasulu Reddy & Solomon Dufera Tolcha, 2019)

VI. Sheet lamination

Sheet lamination, as defined by ASTM, is a 3D printing technique in which material sheets are fused together to form a component of an item (Silbernagel, 2018). Two 3D printing technologies that apply this technique are laminated object manufacture (LOM) and ultrasonic additive manufacturing (UAM) (Tofail et al., 2018). Full-color printing is possible with sheet lamination, it is affordable, handling the material is easy, and extra material may be recycled. Complex geometrical elements may be produced using laminated object manufacturing (LOM) at a lower cost of production and in less time (Shahrubudin et al., 2019). A revolutionary process called ultrasound additive manufacturing (UAM) uses sound to combine layers of metal extracted from a foil sheet without any features. The example of a sheet lamination arrangement is shown in Figure 2.6.

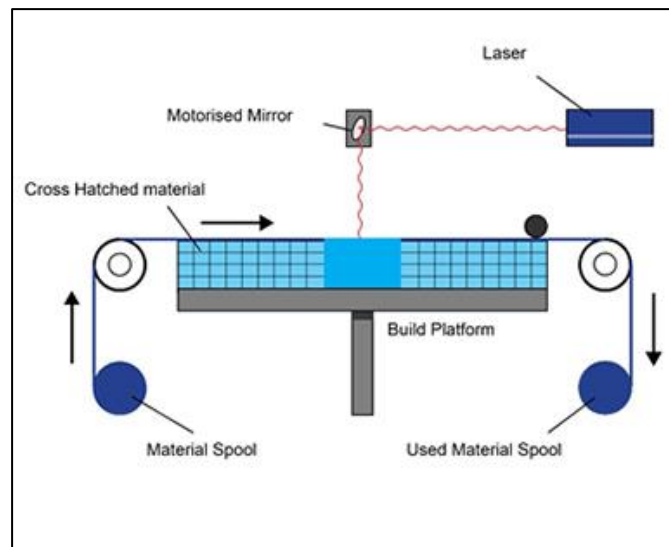


Figure 2.6 Sheet lamination

VII. Vat Photopolymerization

Photopolymerization, also known as the curing of photo-reactive polymers with a laser, light source, or ultraviolet (UV) radiation, is the most widely used 3D printing process (Low et al., 2017). Two examples of photopolymerization-based 3D printing technologies are stereolithography (SLA) and digital light processing (DLP). The SLA was affected by the photo initiator, the irradiate exposure, any dyes, pigments, or extra UV absorbers that were present (Shahrubudin et al., 2019). Comparable to stereolithography, digital light processing is a photopolymer-based technology. The fundamental difference is in the light's source. The Digital Light Process makes use of a more conventional light source, like an arc lamp with a liquid crystal display panel. It is quicker than stereolithography because it may complete the whole surface of a vat of photopolymer resin in a single pass. In Vat Photopolymerization, the exposure time, wavelength, and power source are all important factors. When exposed to UV radiation, the materials used initially as liquids solidify. Photopolymerization is suitable for producing a high-end product with excellent details and a high

degree of surface quality (Ernst & Young, 2016). Figure 2.7 shows the setup for Vat photopolymerization.

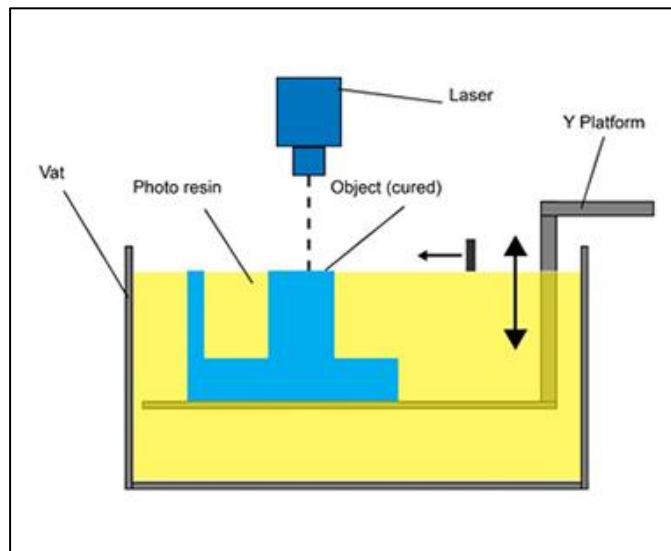


Figure 2.7 Vat photopolymerization(K Srinivasulu Reddy & Solomon Dufera Tolcha, 2019)

2.2.2 3D Printing Technology Application

A synonym for 3D printing is additive manufacturing. Additive manufacturing was utilized for prototyping in the early 1980s, but because of its precision, replicability, and affordable production prices, it has gained favor recently (Shaik et al., 2021). The next paragraphs will discuss some of the industries that frequently employ 3D printing technology, including aerospace, automotive, the food industry, and electric and electrical.

I. Aerospace

The development of 3D printing technology has opened previously unheard-of component and production design freedom. The ability of 3D printing technology to produce lightweight parts with excellent and complicated geometry in the aerospace sector reduces the demand for energy and resources (Joshi & Sheikh, 2015). Utilizing 3D printing technology can also cut down on the material needed

to produce aeronautical parts, which can result in fuel savings. Another typical use of 3D printing technology is the production of spare parts for various aviation components, including aircraft engines. Because they are easily damaged, engine parts constantly need to be changed. Because of this, using 3D printing technology to obtain such spare parts is a terrific idea (Y. C. Wang et al., 2019). The aerospace industry favors nickel-based alloys because of their excellent tensile strength, oxidation/corrosion resistance, and damage tolerance.

II. Automotive

The advancement of 3D printing technology has significantly changed our industry's capacity to produce new goods. The automotive sector has seen considerable breakthroughs because to 3D printing, which allows for faster, lighter constructions of more complicated designs. For instance, Local Motor used 3D printing to produce the first electric vehicle in 2014. By constructing the OLLI 3D-printed bus in addition to cars, Local Motors broadens the scope of applications for 3D printing technology. The OLLI bus is a driverless, electric, highly intelligent, and 3D printed vehicle. In addition, Ford is a pioneer in the use of 3D printing technology, using it to create prototypes and engine parts (Sreehitha, 2017). In order to create faultless and effective automotive designs, firms can test out various options and emphasize them early in the development process by utilising 3D printing technology in the automotive industry. One benefit of 3D printing technology is the potential reduction of material waste and consumption at the same time. Additionally, 3D printing technology can enable speedy testing of innovative ideas while saving money and time (Manghnani, 2015).

III. Food industry

The food industry is being revolutionized by 3D printing technology, in addition to the aerospace industry. Food that is specially created for individuals with specialist dietary requirements, such as athletes, youngsters, pregnant women, and sick, who require a diverse amount of nutrients, is now becoming more and more popular. To achieve this, less unnecessary ingredients and more nutrient-dense ones must be employed (Dankar et al., 2018). However, making customized meals calls for a methodical and creative approach, and here is where using 3D food printing is important. The procedure, also known as "3D food printing" or "food layer fabrication," entails the deposition of consecutive layers using computer-aided design data (L. Liu et al., 2019). It is now feasible to combine and process particular materials into a range of intricate structures and designs by using 3D printing technology (Z. Liu et al., 2017). Innovative culinary dishes with elaborate and alluring designs and forms can be made by combining components like sugar, chocolate, pureed food, and flat foods like spaghetti, pizza, and crackers.

IV. Electric and electronic

Manufacturers are beginning to see the potential of 3D printing realised in a variety of fascinating ways as it becomes more widely accessible in the domains of research, technology, and industry. Making structural electronic devices using various 3D printing techniques is one of these areas. These procedures enable the mass customisation and adaptive design of active electronic materials, electrodes, and gadgets. To accomplish this, conductors are incorporated into the 3D-printed components (J. Lee et al., 2017). The Fused Deposition Modelling (FDM) method of 3D printing, which offers a cost-effective and speedy method for mass-producing electrode materials, is utilised in the manufacturing process for 3D electrodes.

Contrary to industrial electrodes like carbon, copper, and aluminium electrodes, 3D electrodes' shape and surface area are easily adaptable to different uses. Additionally, the 3D printing method used to create these electrodes is completely automated and accurate, making it possible to generate eight electrodes in just 30 minutes (Foo et al., 2018). A wide range of instruments that can amplify and control electric currents are included in active electronic components. Active gadgets also include those that can produce their own electricity. Silicon-controlled rectifiers, transistors, diodes, operational amplifiers, light-emitting diodes (LEDs), batteries, and more are examples of active electronic components. Compared to passive components, these components frequently require more complicated manufacturing procedures because of their variety of capabilities (Saengchairat et al., 2017).

2.2.3 3D printing Filament Material

Today, a variety of filament materials for 3D printing are accessible, each with special characteristics and printing temperatures. The material used to make 3D printing filament is called thermoplastic feedstock, which is a type of plastic or polymer that melts, may be moulded, and hardens when cooled. Plastic is a great 3D printing material since it is environmentally friendly. By melting and layering thermoplastic filaments in FDM printers, plastic things are frequently created (Kristiawan et al., 2021). Some of the most often used 3D printing filament materials are polylactic acid (PLA), acrylonitrile butadiene styrene (ABS), polyvinyl alcohol plastic (PVA), polycarbonate (PC), pure composites like polypropylene, polyethylene terephthalate, and others. In addition, filaments made of composite materials combined with natural fibers are employed in 3D printing. The addition of natural fiber to thermoplastic is a reinforcing material that enhances the mechanical

properties' thermal stability, extending the working temperature and enhancing the consistency of material behaviors at both high and low temperatures. On the other hand, advances in 3D printing have given the opportunity to recycle thermoplastics as a feedstock material for 3D printing (Kristiawan et al., 2021).

2.3 Polypropylene as Matrix in Composite

A C₃H₆ polymer used in the manufacture of plastics is polypropylene (Shubhra et al., 2013). It can be used as a structural plastic or a fibre, and it has many uses in both industrial and consumer goods. Food containers made of this plastic are frequently produced, especially those that need to be dishwasher safe. Polypropylene has a relatively high melting point of 320°F (160°C) in comparison to other polymers (Shubhra et al., 2013). Polyethylene, another common container material, has a much lower melting point (Shubhra et al., 2013). Even though polypropylene is renowned for being both lightweight and very durable, the texture of the substance varies according on the method of polymerization used (Shubhra et al., 2013). Define isotactic polypropylene as a stiff polymer made of methyl group atoms bonded to one side of an atomic chain. Figure 2.8: Polypropylene's atomic chain.

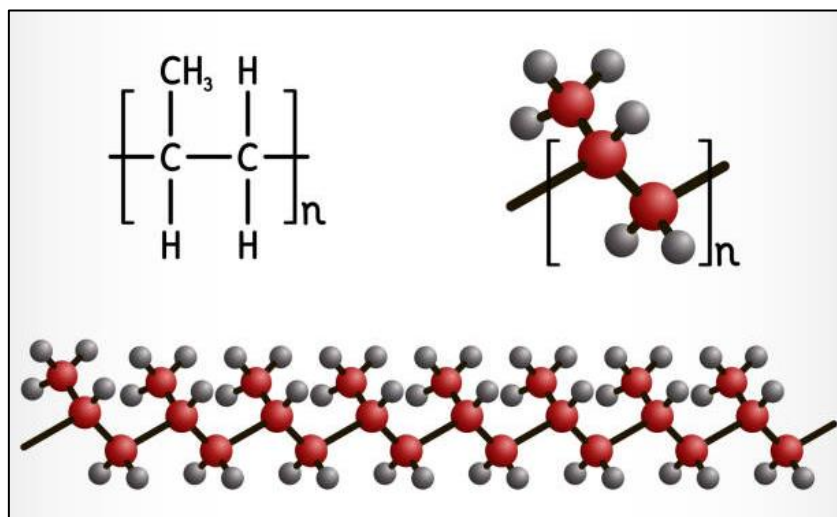


Figure 2.8 Polypropylene's atomic chain.

2.3.1 Recycled Polypropylene

Waste polypropylene is separated from other types of resins during mechanical recycling. It goes through a washing process to get rid of debris and impurities, then is ground and crushed to make the particles smaller. The material is then reprocessed and heated extruded to create new plastic products. The breakdown of plastic trash into its original monomers or other valuable components occurs during chemical recycling. With this method, the plastic is intended to be reduced to its fundamental components for future usage. As an alternative, the burning process used in the incineration of plastic garbage produces energy. Although this process does not directly recycle the plastic, a result of it is the production of electricity (Morales et al., 2021). Recycling processes that use mechanical and chemical processes are the most common ones used to handle polypropylene waste. In the plastics sector, which mainly relies on oil and has important environmental and economic ramifications, polypropylene recycling and recovery rates are crucial. The industry may decrease its reliance on oil, lessen its negative effects on the environment and the economy, and increase the reuse and recovery of recycled polypropylene (Morales et al., 2021). Consequently, a number of advantages result. First, there is a decrease in the amount of energy and raw resources, such as propylene, required to make new products. A more effective utilisation of resources results from this. Second, recycling contributes to sustainability by reintroducing a sizable percentage of raw materials into the economic cycle. Third, the total amount of polypropylene waste being burned or dumped in landfills is decreased, lowering the environmental effect of waste disposal. These beneficial effects can be attained by putting into practice efficient recycling procedures (Morales et al., 2021).

2.3.2 Recycled Polypropylene Properties and Application

Every piece of plastic has a Resin Identification/Plastic Recycling Code that is unique to the type of resin used. Polypropylene's resin identification number is 5, according to Van de Velde from 2002. Collecting, sorting, cleaning, reprocessing, and producing new goods are the five steps in the recycling of polypropylene (Morales et al., 2021). Separate the polypropylene first, then the other plastic polymers. The "sink float" separation process is used to do this, and it relies on the particular specific density of polypropylene (0.93-0.95 g/cm), which causes it to float while other polymers, such as PET (specific density 1.43-1.45 g/cm), sink (Morales et al., 2021). After melting polypropylene in an extruder at temperatures above 400 degrees Fahrenheit, granulation for use in new manufacture occurs (Martín-Alfonso et al., 2013). Polypropylene's hydrogen-carbon bonds gradually degrade thermally, lowering the plastic's structural intensity (Momanyi et al., 2019). To remove impurities, waste plastic is heated to a temperature of about 250 degrees Celsius, vacuum extracted to remove any remaining molecules, and then solidified at a temperature of about 140 degrees Celsius (Momanyi et al., 2019). Recycled polypropylene can replace up to 50% of this virgin polypropylene. Recycled polypropylene is utilised in packaging materials, automobile bumpers, foams, bottle caps, carpets, and candy wrappers in addition to straws and candy wrappers. Typically, bitumen percentages of 2 to 5% by mass are employed for bitumen asphalt applications (Morales et al., 2021). The filament for 3D printing may also be made from recycled polypropylene.

2.4 Wood Fiber as Reinforced Material in Composite

2.4.1 Wood Fibre Physical and Mechanical Properties

Wood falls under the lignocellulosic category. Ash and extractives are minor components, while cellulose, hemicellulose, and lignin are the three main ones (Laurent M. Matuana, 2015). The majority of the combination is made up of structural elements with high molecular weight. Wood contains between 60 and 75% cellulose, 20% lignin, 10% extractives, and 4% ash. Each of details wood content is described below:

I. Cellulose

The most prevalent organic compound is known to be cellulose, which is the main structural element of wood. The linear structure of the cellulose molecule is determined by how the β -D-glucose units are arranged. These components are linked together to form lengthy chains that are arranged in a single plane and are made up of atoms of carbon, hydrogen, and oxygen (Matuana & Stark, 2015). The hydroxyl groups on cellulose's surface are responsible for its reactivity. These hydroxyl groups have the capacity to join water molecules via hydrogen bonds. Because cellulose is polar, it easily forms hydrogen bonds with water, giving it its hygroscopic qualities (Marra, 1992). Figure 2.9 shows the structure of cellulose.

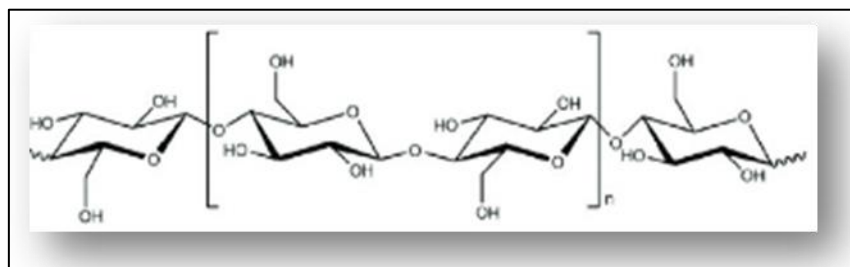


Figure 2.9 Structure of cellulose(Ndibewu & Tchieta, 2018)

II. Hemicellulose

Similar to cellulose, hemicellulose is made up of sugar chains with five or six carbon atoms each. The chains, however, can be broken down into a more soluble state or dissolve quickly because they are short enough (Marra, 1992). The polymerization degree is only made up of tens or hundreds of repeating units (Kazayawoko et al., 1999). Hemicellulose content is higher in hardwoods than in softwoods. Figure 2.10 shows the structure of hemicellulose.

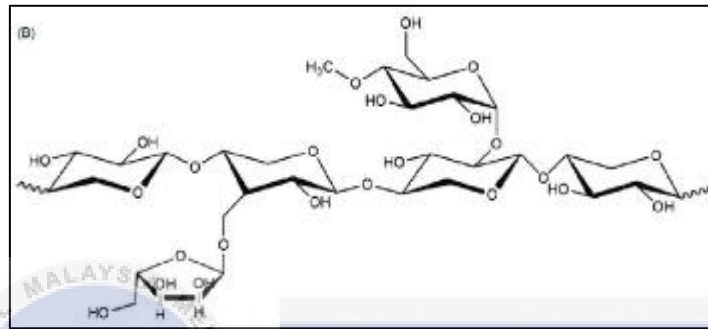


Figure 2.10 Structure of hemicellulose(Ndibewu & Tchieta, 2018)

III. Lignin

The cellulose fibres are held in place by the lignin that serves as a matrix in plant cell walls. It serves as a bonding and stiffening agent and is fragile and relatively inert. The matrix and the fibre can transfer stress to one another thanks to lignin's capacity to diffuse into the fibre wall and increase stiffness. About 23–33% of softwoods and 16–25% of hardwoods contain lignin, with the former being more prevalent (Matuana & Stark, 2015).

Additionally present in lignin are carbon, hydrogen, and oxygen. A phenolic chemical served as the starting point and was subjected to a number of combinations to produce a highly branched three-dimensional network. As a result, an isotropic material is created. The six-member rings of lignin are totally made of carbon atoms, and they resemble benzene rings in that they include a small number of hydroxyl groups. Given how reactive cellulose is, lignin is much less so (Matuana & Stark, 2015). Figure 2.11 shows the structure of lignin.

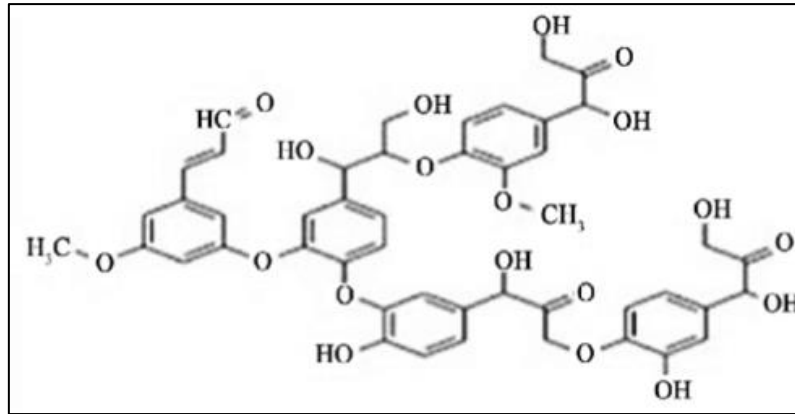


Figure 2.11 Structure of Lignin(Muktham et al., 2016)

As significant as the material properties listed are, the context of the wood's intended use must also be considered. Due to the fact that wood is a viscoelastic material, its mechanical properties fluctuate with time. Additionally, when exposed to higher temperatures or more moisture, wood's mechanical performance often deteriorates (Bao et al., 2001). The mechanical characteristics of structural wood are significantly harmed by global fibre deviations like spiral grain and local fibre misalignment around knots. Except for the purest form of the material, practically all examples of wood contain these alterations and misalignments. These imperfections may weaken and inconsistently affect the wood's overall structural integrity and strength (Olsson et al., 2013). For the reason, Table 2.2 of EN 338, which lists typical values for mechanical properties of lumber, provides far lower values than those found for small faultless specimens.

Table 2.2 Selected characteristic values for soft- and hardwood according to EN 338(Olsson et al., 2013)

Property	Softwood					Hardwood				
	C14	C20	C27	C40	C50	D18	D30	D50	D65	D80
Tensile strength (5% fractile)	7.2	11.5	16.5	26	33.5	11	18	30	39	48
Modulus of elasticity (mean)	7	9.5	11.5	14	16	9.5	11	14	18.5	24

Transverse compression, the most often employed method for wood densification (Jakob et al., 2022), allows for a large reduction in cell void volume in Figure 2.12 (a). Compression takes place when the amorphous polymers within wood reach a sufficient level of flow. The compressed wood is then put through a drying process to promote hydrogen bond formation and increase dimensional stability. Fixation, the process' last phase, tries to keep the wood in its compressed state so as to ensure long-term stability and endurance (Morsing, 1998). It's interesting to note that both high humidity and high temperatures help wood to compress. The densification attained under these conditions can be largely regained when wood is subjected to high humidity levels once more. This indicates that under these particular environmental circumstances, the wood can recover most of its initial density and strength (Jakob et al., 2022). Diverse densification techniques have been created since the turn of the 20th century to enhance the mechanical qualities of wood while reducing set recovery. By obtaining higher densities, recent improvements in mechanical processes have surpassed simple scaling. These developments have produced more complex techniques for wood densification, enabling the improvement of mechanical properties without sacrificing the wood's capacity to regain its former shape and dimensions, according to Figure 2.12. The mechanical characteristics of densified wood products produced using different processes are summarised in Table 2.3. It should be noted that Table 2.3 contains both tensile and bending data, depending on how the densified material was described in the relevant experiment. A material is subjected to a complex interaction of tension, compression, and shear forces during bending. In the case of solid wood, the bending strength typically does not exceed its tensile strength. This means that the wood's ability to withstand tension is generally greater than its resistance to bending forces (Jakob et al., 2022) and may thus be seen as a lower limit for the latter. The most important procedures for wood densification, as well as the resulting mechanical qualities, are briefly detailed here.

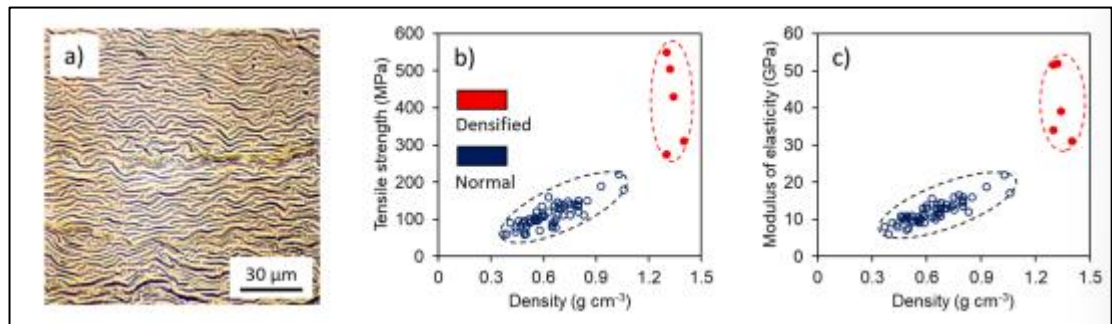


Figure 2.12 Microscopic structure of densified wood (a) and comparison of the variability of tensile strength (b) and modulus of elasticity (c) of normal and densified wood, respectively (Jakob et al., 2022)

Table 2.3 comprises both tensile and bending data

Wood species	Density (g cm ⁻³)	Tensile strength (MPa)	Modulus of elasticity (GPa)
Thermo-mechanical (TM) compression			
Laminated yellow birch	1.4	310	32
Laminated sweetgum	1.36	225	26
Laminated Sitka spruce	1.36	325	36
Spruce	0.99	185	31
Viscoelastic thermal compression (VTC)			
Hybrid poplar	0.79	155 ¹	20
Laminated radiata pine	0.65	175 ¹	18
Polymer-infiltrated compressed wood			
Laminated spruce	1.3	275	28-35
Laminated yellow birch	1.34	210	26
Laminated sweetgum	1.35	185	21
Laminated Sitka spruce	1.34	165	30
German spruce, Douglas fir, Japanese birch, Jatoba	1.3-1.4	300-500 ¹	-25-50
Delignified compressed wood			
Spruce	-	±270	-35
Bass	1.3	550	52
Pine	1.32	720	19
Basswood	1.2	350	33
Spruce	0.83	310	21
Delignified and partially fibre surface dissolved compressed wood			
Birch	-1.35	-430	-39
Birch	-1.25	-370	-46
Delignified resin-infiltrated compressed wood			
Laminated hoop pine	1.4	455 ¹	39
Laminated German spruce	1.4	670 ¹	62
Laminated Japanese cedar	1.15	280 ¹	27
Norway spruce	1.32	505	52
Norway spruce	1.32	420 ¹	47
Basswood	0.92	330	-

¹...bending properties.

2.4.2 Example of Wood Fiber Application as Reinforced Materials

Wood-Plastic Composites (WPCs) have grown significantly in popularity over the past ten years as a commercial product in a number of sectors, including construction, transportation,

furniture, and consumer goods. The adoption of WPCs in the building sector has been the main factor in the commercialization of WPCs in North America. WPCs are being used in many different items, including decking, railing, window and door lineals, roofing materials, picnic tables and benches, fencing, landscape timbers, patios, gazebos, pergolas, automobile parts, and playground equipment. These instances demonstrate the various and growing applications of WPCs across several industries (Matuana & Stark, 2015). The author claims that the development of furniture applications and the use of WPCs for interior panel parts have both been heavily influenced by the European car sector. Asian producers, on the other hand, are mostly focused on the furniture industry and use WPCs for applications like as interior construction and aesthetics. This demonstrates the regional differences in the use and emphasis of WPCs in the furniture and automobile industries. According to the study that was done by (Crespell, 2008) It is anticipated that WPC adoption would rise across a number of market categories in North America. Siding, fencing, bridge decking, foundation isolation components, marine structures (like chocks, wales and pier decking), laminate flooring, household furnishings (like bathroom/kitchen cabinets and patio furniture), utility poles, railway ties and exterior and interior moulding and millwork are some of these segments. Injection moulding is also anticipated to offer up new markets for toys and the packaging of cosmetics as it becomes more popular for WPCs. The market for injection-molded auto parts, such as glove boxes, fastening hooks, sound systems, and fan boxes, is predicted to grow in Europe. These observations give a general overview of the prospective growth opportunities for WPCs across several geographies and sectors (Carus et al., 2008). WPCs are expected to expand in popularity as a result of current research and development projects aimed at improving their performance, particularly for structural applications. In order to increase the strength, stiffness, and creep resistance of WPCs, many methods are being investigated. Reactive extrusion is one such technique, which includes crosslinking

the polymer matrix of WPCs with silanes. The WPC materials become more durable, tougher, and have less creep as a result of this technique. The increased potential for WPCs as structural elements is a result of these developments in material composition and manufacturing methods (Bengtsson et al., 2007). Based on (Matuana & Stark, 2015), Incorporating nanoparticle-reinforced polymers into the matrix is another way to improve the structural performance of WPCs. The strength and stiffness of the WPC composition can be greatly increased by adding nanoparticles. It is also becoming more popular to combine WPCs with non-WPC materials, which enables the development of structural composites that are more adaptable. Several Chinese WPC producers are already extruding WPCs over solid metal or solid wood, enabling the fabrication of structural components with WPC surfaces that mimic nonstructural members' look. This method works especially well in structures like pergolas and gazebos where both structural soundness and aesthetic appeal are important. WPCs can offer practical and aesthetically uniform solutions in structural composite applications by fusing several materials.

By substituting different chemical groups for some of the hydroxyl groups, wood's hygroscopicity, or propensity to absorb moisture, can be decreased. Research on acetylation in particular has focused on enhancing the moisture performance of wood and wood composites. Acetylated fibres are created when acetic anhydride combines with the hydroxyl groups found in the cell walls of wood during the acetylation process. For instance, when pine wood fibres are acetylated, the equilibrium moisture content is significantly reduced, going from 22% to 8% at 90% relative humidity and 27°C. By altering the composition of the wood, this acetylation procedure can improve the dimensional stability and decay resistance of the material while also lowering its sensitivity to moisture absorption (Abegunde et al., 2020) Less extensively, the acetylation method has also been investigated to give Wood-Plastic Composites (WPCs) moisture resistance. A WPC composite that

contained 50% wood fibre and 50% polypropylene (PP) was found to absorb 5% moisture after 34 days of soaking in a study. However, the moisture absorption was dramatically decreased when the wood fibres were acetylated before being added to the WPC composite. Under the same circumstances, the 50% acetylated wood fibre loaded PP composite only absorbed 2.5% moisture. According to this study, wood fibres used to make WPCs can be efficiently acetylated to increase their moisture resistance, making them better suited for applications where moisture exposure is a problem. Acetylated wood fibre packed WPC composites can display improved dimensional stability and durability by minimising moisture absorption (Khalil et al., 2002).

2.5 Maleated Anhydride Polyethylene Coupling Agent

When reinforcing composites with fillers and fiber reinforcements, maleated coupling agents are frequently used (Khalid et al., 2021). The incompatibility issue can be resolved by using interactions between the hydroxyl groups of natural fibers and the anhydride groups of maleated polymer additives to increase the tensile strength of fiber thermoplastic composites (Zakaria Razak et al., 2018).

Maleated coupling agents with the ideal balance of maleic anhydride and molecular mass can generate the optimum performance in fiber composites, according to actual property data (Keener et al., 2004). With regard to wood fiber/high density polyethylene (PE) composites, the effectiveness of oxidation polyethylene, MAPP, and newly discovered maleated polyethylene (MAPE) combiners is explored (Hao et al., 2021b). The addition of 1-5% MAPE or MAPP to WPCs can result in a 30-100% improvement in mechanical characteristics (Hao et al., 2021b)

To overcome weak interfacial bonding, maleated polyolefins (MAPE or MAPP) are often employed as appropriate polymer additives in WPCs (Hao et al., 2021b) MAPE couplers, which were recently discovered, have been shown to improve both the tensile and stress properties of wood/HDPE composites significantly more than other potential polyolefin couplers (Keener et al., 2004). Figure 2.13 shows the chemical bonding of Polyethylene-graft-maleic anhydride (PE).

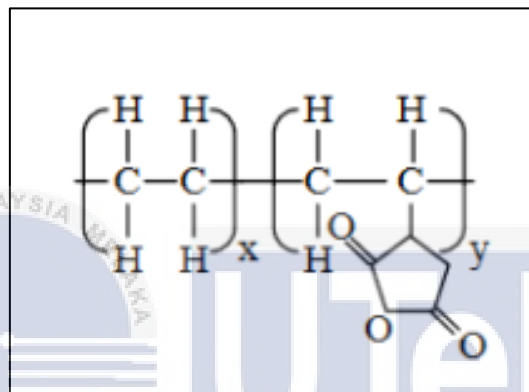


Figure 2.13 Polyethylene-graft-maleic anhydride (PE)

2.6 Summary of Literature Review

To summarize, there is a wealth of relevant information gleaned from prior studies on the MAPE effect on WPC filament in 3D printing. The findings of this literature study cover the history and method of FDM 3D printers, as well as 3D printing. Printing material, natural fiber 3D printing material, composite 3D printing filament type, and filament processing. All this information was acquired and will help with this research, which is a study of the influence of MAPE on the 3D printing filament qualities created from WPC.

CHAPTER 3

METHODOLOGY

3.1 Introduction

This chapter outlines the research methods used to carry out the study in detail. Research methods presented in this chapter were performed to achieve the objectives of the study.

Figure 3.1 shows the flow of the research methodology.



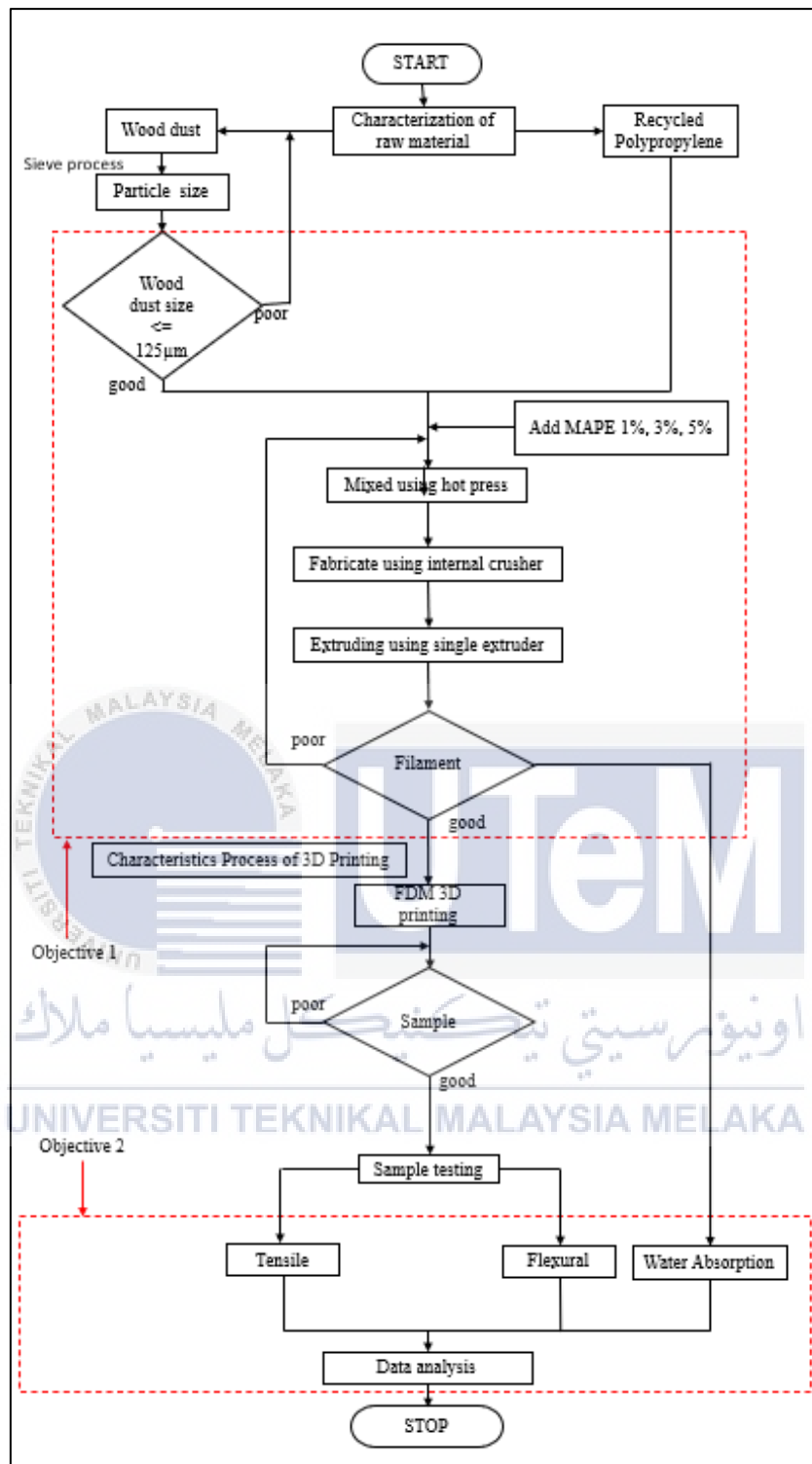


Figure 3.1 The flow of the research methodology.

3.2 Preparation of Material

3.2.1 Recycled Polypropylene (rPP)

The recycled polypropylene (rPP) was used in this study was in Pallet condition. The total that we used is the composite loading, which is 500g per sample. This rPP was ordered from a supplier for the purpose of this study and is in good condition to undertake this experiment.

Figure 3.2 shows the raw material of recycled polypropylene.



Figure 3.2 the raw material of recycled polypropylene.

3.2.2 Wood Dust

Recycle wood dust fiber that have buy from online platform Shopee. Figure 3.3 show the raw material of the wood dust.



Figure 3.3 show the raw material of the wood

The wood dust fibre (WF) used in this investigation was washed with distilled water to remove dust and dried in an oven at 80°C to ensure a moisture content of less than 3 wt.%, as described by (Fu et al., 2021). The dried WF was sieved using a sieving machine, as shown in Figure 3.4. This study made use of wood dust fibre with particle sizes of 125 μm .

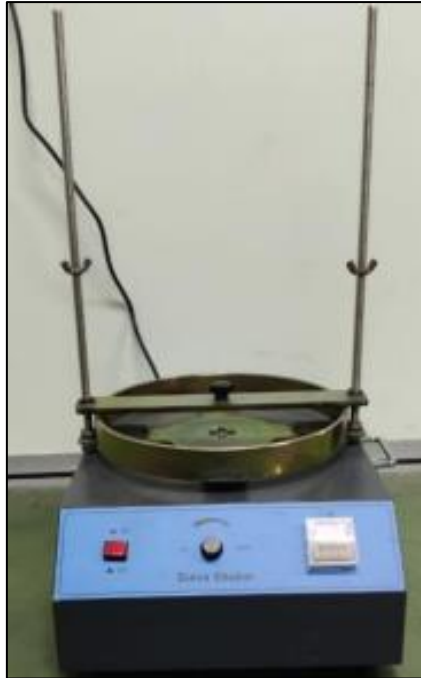



Figure 3.4 Sieving Machine

To assess the particle size of wood dust, the sieve technique is utilised. In this experiment, wood dust with particle sizes of 125 μm or less was employed. Wood particles, unlike spherical spheres, are non-spherical. Because their morphologies include particles, coils, and chips, fluidizing these systems is unlikely. Getting a sieve with a mesh size of 125 microns is the first thing that needs to be done. Check that the sieve is spotless and in good shape before using it. The wood fibre should then be prepared. The sieve should be placed on top of the container or tray that is being used for collection, and it should be positioned in such a way that it is firmly in place. After that, the process of sieving ought to get underway. This can be conducted manually by gently shaking the sieve, or it can be accomplished with the help of mechanical sieving equipment. Both methods are viable options. After going through the sieve mesh, the particles that are smaller than 125 microns will be allowed to aggregate in the container that is located below. After a period of thirty minutes, the machine will stop working on its own. Following that, wood dust was added to the bag. Following that, the process was repeated when the target was archived. Table 3.1 shows sieving process.

Table 3.1 Step in Sieving process

No	Process	Figure
1	The washed wood dust had been prepared.	 <p>The figure shows two large, clear plastic bags filled with a fine, brown, granular material, which is the washed wood dust. The bags are stacked one on top of the other.</p>
2	The sieve machine was set up correctly.	 <p>The figure shows a mechanical sieve machine. It has a blue base with a control panel featuring a red power button, a black dial, and a white switch. A circular sieve is mounted on top of the machine, held in place by a metal frame.</p>

3	<p>The sieves of three different sizes were on hand. which is: - i. 0.3mm ii. 0.2mm iii. 0.125mm. This configuration will be utilised in the sieve procedure to determine the precise particle size.</p>	
4	<p>The 125 m sieve was utilised for the final screening of the wood dust fibre.</p>	
5	<p>The siver machine was turned on and a 10-minute timer was set. This procedure was repeated until the weight of the wood fibre was determined.</p>	

6	The 125 μm particle size of wood dust fiber was prepared for the composite fabrication.	
---	--	--

3.2.3 NaOH Solution

For this research, the sodium hydroxide (NaOH) solution was applied as a liquid for the treatment of the wood, in Figure 3.5 and Table 3.2 provided product specifications.



Figure 3.5 NaOH on Liquid Form

Table 3.2 Specification of Sodium Hydroxide

Items	Specifications
Physical Form	Liquid
Colour	White
NaOH Content	More than 99%
Water Solubility	100%
Molecular Weight	40g/mol

wood fibre composites frequently use the quick and easy alkali (NaOH) treatment method to modify their surfaces. Table 3.3 displays the weight ratio for water. Alkali (NaOH) treatment was proven to improve tensile and flexural properties while decreasing impact strength (Radzi et al., 2019). NaOH solution will be prepared in this study using 6% NaOH concentration and 94% H₂O to get the 100% mixture for NaOH solution in Figure 3.6.

Table 3.3 Weight Ratio of Water

No	Material	Amount(g)	Amount(%)
1	NaOH	60	6
2	Water	60	94
3	Total	120	100



Figure 3.6 NaOH Solution

3.2.3.1 NaOH treatment of Wood Dust Fibre

Sodium hydroxide (NaOH) solution is the alkaline treatment method used for wood dust fibres because of its immediate impact on cellulosic fibrils, extraction of lignin and hemicellulose components, and simplicity of processing. When sodium hydroxide's hydroxyl group interacts with cellulose, swelling and a loosening of the fibre structure result, making the material more accessible. By reducing ester bonds as a result of a reaction with sodium hydroxide, lignin extraction is made easier while also increasing purity and fibre characteristics. By hydrolyzing glycosidic linkages, which lowers the amount of hemicellulose and increases the amount of cellulose, hemicellulose molecules can be recovered. The procedure is popular for industrial applications because it is straightforward and inexpensive and because the alkaline conditions produced by sodium hydroxide improve the quality and suitability of the treated wood fibres for a variety of industries (Nadlene et al., 2018).

The wood dust fibres underwent an alkaline treatment procedure by being soaked in a 6% sodium hydroxide (NaOH) solution for two hours at room temperature. NaOH treatment shown in Figure 3.7. The NaOH solution's hydroxyl group interacted with the cellulosic fibrils during this phase, causing them to enlarge and the fibre structure to loosen, improving their accessibility for subsequent processing. The alkaline conditions also made it easier to extract lignin and hemicellulose from the wood fibres because the hydroxyl group reacted with the ester linkages in lignin and hydrolyzed the glycosidic bonds in hemicellulose. The treatment time provided for the best responses and adequate NaOH absorption (Nasereddin et al., 2018).

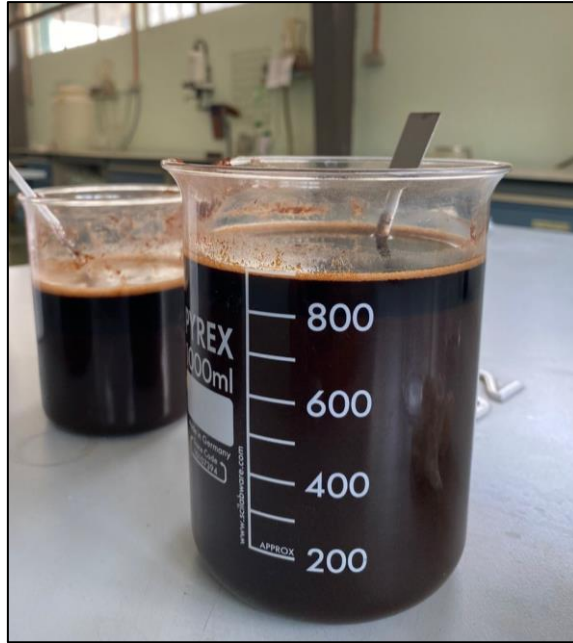


Figure 3.7 NaOH Treatment

The wood fibres were carefully rinsed several times with running distilled water after the alkaline treatment procedure. This washing process was essential for getting rid of any contaminants and leftover sodium hydroxide solution from the treated fibres. The fibres were thoroughly cleaned and prepared for further processing thanks to the frequent washing.

Figure 3.8 shows cleaning process of the wood fibre.



Figure 3.8 Cleaning Wood Fibre using Distilled Water

Following the washing procedure, the wood fibres were dried for 24 hours in an oven at a controlled temperature of 60 °C (Kumar et al., 2018). Figure 3.9 shows the drying process. By drying the fibres at this particular temperature, moisture could be removed while the danger of overheating the fibres was reduced. The drying procedure made sure the fibres attained the ideal moisture content for their intended uses.



Figure 3.9 The Drying Process

3.2.4 Preparation of MAPE

Maleated anhydride grafted polyethylene (MAPE) as agent coupling was purchased in pallet form. Figure 3.10 shows the example of MAPE.

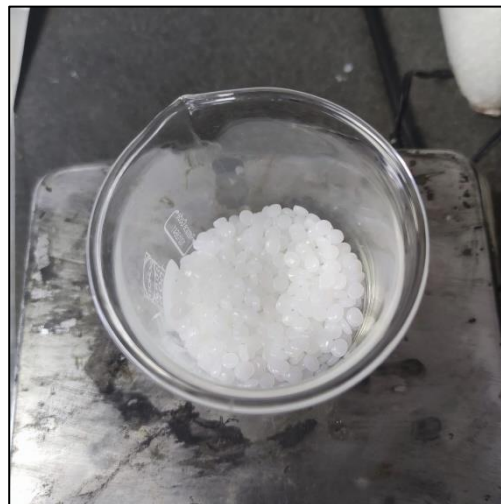


Figure 3.10 shows the maleated anhydride grafted polyethylene (MAPE)

The MAPE additive was weighed using a scale in accordance with the ratio that was chosen. Because of its pellet form, the preparation must be more meticulous.

3.3 Fabrication of Filament

3.3.1 Preparation of Recycled Polypropylene/Wood Dust/MAPE Composite

Wood dust fibre with varied composition (3% wt.) was extensively pressed by MAPE containing at various composition (1%, 3%, and 5% wt.) with recycled polypropylene to fabricated with hot press process. It was developed in a lab located in the manufacturing department of the Faculty of Technology. First came the recyclable polypropylene, then the wood dust fibre, and ultimately the MAPE. Table 3.4 shows the amount of wood dust fibre, recycled polypropylene (PP), and MAPE used in this study.

Table 3.4 The amount of wood dust fibre, recycled polypropylene (PP), and MAPE

Sample Identification	Wood dust fiber	Recycled PP	MAPE
0	3% = 5.76g	794.24g	0% = 0g
1	3% = 5.76g	786.08g	1% = 8.16g
2	3% = 5.76g	769.76g	3% = 24.48g
3	3% = 5.76g	753.44g	5% = 40.8g

3.3.2 Hotpress Process

The process of mixing PP, MAPE, and WF using the hotpress approach involves a number of different activities. The combination of polypropylene and treated ground tyres is accomplished by the hotpress process, which is comprised of several operations. The PP, WF, and MAPE are cleaned up and prepared for use at a later time during the first step of the procedure. After that, the rubber and the polypropylene (PP) are thoughtfully mixed together in order to ensure that the rubber particles are spread uniformly throughout the PP. In order to facilitate the melting and flow of the polypropylene (PP), the combined material is then heated to a specific temperature afterward.


The mixture is placed between two heated plates or moulds once the hotpress machine shown in Figure 3.11 is ready to serve its purpose. After the polypropylene (PP) is heated to the point where it melts and flows, but not to the point where it become degraded, it is then subjected to pressure that is uniform throughout the entire surface. This promotes the embedding of the WF and MAPE particles in the molten PP, which in turn improves the connection between the two types of particles.



Following the application of heat and compression for a predetermined period of time, the material is then subjected to a gradual cooling process while the pressure remains unchanged. During the cooling process of the composite material, the WF particles become sufficiently distributed throughout the PP matrix. Following the completion of the curing process, the composite material is removed from the moulds and allowed to cool to room temperature. In addition to cleaning, cutting, and moulding Table 3.5 provides a visual representation of the step for hotpress process.






Figure 3.11 Hotpress Machine

Table 3.5 Hotpress process

No.	Process	Figure
1	polypropylene, MAPE, and wood fibre was prepare with the value of weight needed.	 <p data-bbox="1034 1496 1134 1525">MAPE</p>

		 <p data-bbox="1011 663 1161 696">Wood fibre</p>  <p data-bbox="1002 1285 1171 1319">Recycled PP</p>
2	<p data-bbox="316 1361 756 1543">Combine MAPE, rPP, and WF in a single packaging beg. The ratio weight refer Table 3.4.</p>	

3	<p>The packaging bed was shaken for a few minutes in all directions to ensure that it was fully mixed before going into the hot press.</p>	
4	<p>For the hot press process, the mould and two stainless steel plates were prepared. The mixture of was inserted into the mould. The composite has been applied to the entire mould, and stainless steel plates were used to shut the top and bottom sides of the mould to prevent the composite from leaking out.</p>	

5	<p>The hotpress was used to lay the mould. A glove was worn for protection and safety.</p>	
6	<p>The hot press was programmed with the following parameters. Initially, the mixture was heated to ensure that the composite was thoroughly mixed. The cooling procedure was used after the hot process to harden the combined composite.</p>	

		
7	<p>The mould was removed from the hotpress machine, and the composite was taken to the pallet crush process.</p>	

UNIVERSITI TEKNIKAL MALAYSIA MELAKA

3.3.3 Crusher Process


After that, the cool composite will be subjected to a crushing process in order to transform it into a pellet. In order to guarantee that the pellet size falls within the allowed range, this procedure will be carried out by means of two or three separate instances. A different kind of crusher machine is depicted in Figure 3.12. The material that has been crushed is brought into the crusher by means of a hopper, a conveyor, or some other type of feeding system. As demonstrated in Table 3.6, the size and type of material that may be utilised can range from rocks to items that have been recycled.






Figure 3.12 the type of crusher machine.



Table 3.6 Crush Process

No.	Process	Figure
1.	Prepare the composite and check that the size of the plate composite is appropriate for entering the crusher machine.	

2.	Place the composite in a machine.	
3.	Take the pallet out of the machine.	
4.	The pallet form is now ready for the next step. If the size of the pallet particle remains large, repeat steps 1-3 one or two more times.	

3.3.4 Extrusion Process

The filament was created using a single extruder, as shown in Figure 3.13 below.

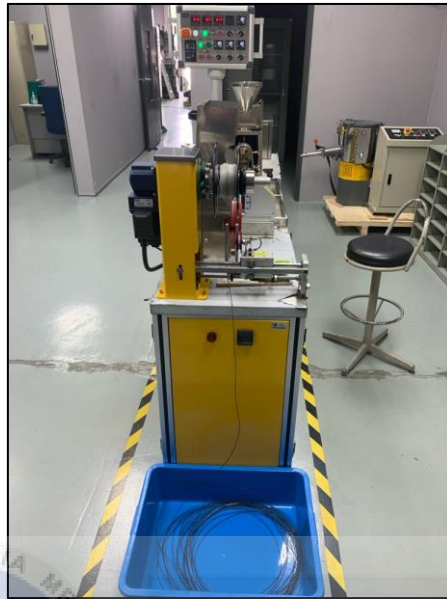


Figure 3.13 Single extruder machine

A single screw extruder with a 1.75 mm die nozzle that fed the filament into three heating zones was used to create the composite material. The barrel and die nozzle zones required initial preheating temperatures of 180°C, respectively. Before being inserted into the hopper, the composite material needs to be heated. In addition, the barrel screw's forward spin (200rpm) was pushing the molten material upward to its die nozzle. The feed cooling zone was also set to a cold temperature to pre-warm the pellets/mixture. A predetermined weight of composite material was fed into the barrel for each feeding interval when the predetermined temperatures for the production of composite filaments were reached. The hot extruded filament was driven through a water-cooled bath by rollers that were tuned to a speed of 10–20 rpm. Additionally, several cooling techniques used during extrusion, such as a cooling water bath, were examined (Figure 3.14) (Polline et al., 2021). The extruded filament needed to be wound into the spooler, where it was loaded onto the rollers for filament storage and spooled at a speed of 16 mm/s (Figure 3.15). The adjustments made to

the filament extrusion processing parameters to maintain the filament diameters within acceptable ranges are summarised in Table 3.7.



Figure 3.14 cooling water bath



Figure 3.15 filament traction rollers

Table 3.7 The filament extrusion processing parameters.

Categories	(r-WoPPc) Filament
	Value
Barrel Temperature (°C)	180
Die/nozzle Temperature (°C)	180
Screw extrusion speed (rpm)	221
Filament pulling roller speed (mm/s)	18

3.4 3D Printing Process

The filaments used in the study were 3D printed using an FDM (Fused Deposition Modeling) 3D printing equipment, as shown in Figure 3.16. The open-source software Ultimaker Cura 4.8.0 was utilized to generate (.stl) files for printing. The CAD model of the standard tensile test specimen Type 1, ASTM D638, ASTM D790 was designed using Solidworks 2021. Five tensile test samples were printed using the composite filaments. For the r-WoPPc filaments, printing nozzle diameters of 0.4 mm and 0.6 mm were employed. Table 3.8 provides the specific printing settings, including a printing strategy of 197°C and 100% infill. To print the filaments, a nozzle temperature of 180-220°C and a bed temperature of 85 °C were used. The filament was fed through a 1mm needle at a speed of 20m/min, resulting in a layer thickness of 0.30mm when the filament reached its melting point. However, the first layer of the 3D-printed specimens encountered issues in adhering to the printer build plate. To address this, commercially available PP filaments are often made with a blend or composite to minimize warping. In this study, despite using Pritt adhesive and Kapton tape, the first print layer did not adhere properly to the printer bed, leading to the premature termination of the printing process (Kristiawan et al., 2022).

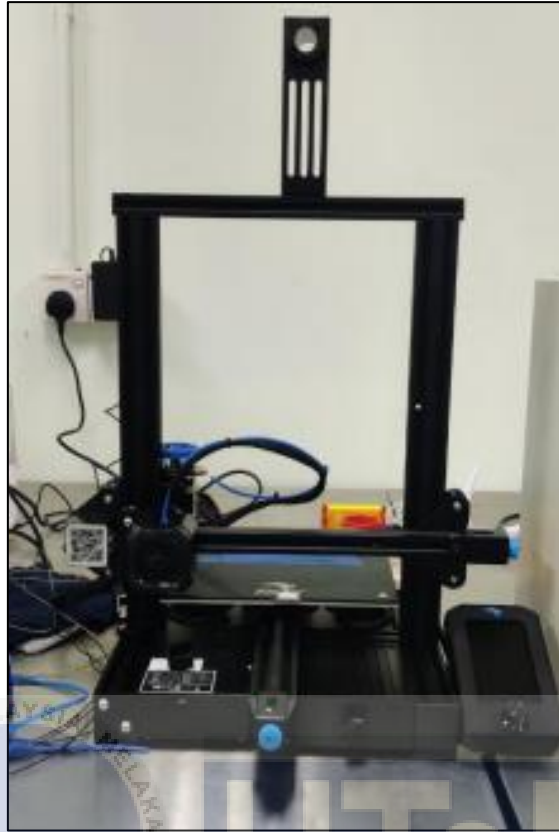


Figure 3.16 FDM 3D printing

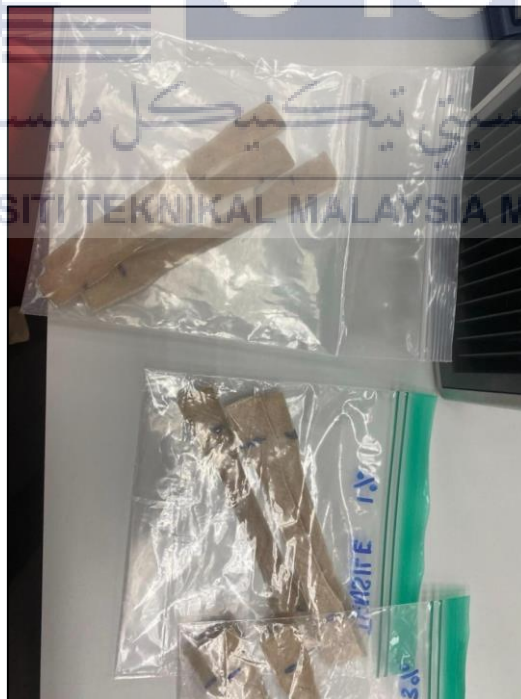


Figure 3.17 Type of specimen

Table 3.8 Printing settings

Parameters	Values
	(r-WoPPc) Filament
Temperature of printing (°C)	197
Initial layer temperature (°C)	197
Build plate temperature (°C)	70
Build plate temperature, initial layer (°C)	70
Infill pattern	Zig Zag
Infill flow (%)	100
The height of the layer (mm)	0.3
Line width (mm)	0.38
Top and bottom layers (layers)	2
The print speed (mm/s)	100
The speed of initial layer (mm/s)	15
Build plate adhesion type	Brim

3.5 Physical Properties (Water Absorbtion)

In line with the filaments, the composite specimens used to test water absorption behavior were immersed in distilled water at room temperature. Before testing, the composite specimens were dried for 24 hours to achieve a consistent weight. The dried samples were soaked in water for 30 days at room temperature. The water intake (percentage) was calculated by dividing the absorbed water weight by the specimen's dry weight. As shown in the following equations in Figure 3.18.

$$\text{Water Absorption \%} = \frac{\text{weight after immersion} - \text{weight before immersion}}{\text{weight before immersion}} \times 100\%$$

Figure 3.18 Equation of Water Absorption

A total of four samples of filament, each measuring 2.5 centimetres in length, were established in order to carry out an experiment involving water absorption. To remove any moisture that may have been present, these samples were subsequently dried in an oven at a temperature of 110°C for a period of twenty-four hours. Figure 3.19 shows the oven used to dried specimen. Because this is the only approach that can guarantee that the filament itself will remain dry, it is the only available option. After the sample had been dried, the initial weight of the sample, which was depicted by the symbol W_i , was determined before the sample was exposed to water. The entire sample was then placed in a room and left there for twenty-four hours after being submerged in distilled water. After that, it was kept. The samples were removed from the container very immediately after twenty-four hours had passed, and a microfiber hand towel was utilised in order to remove any water that was still present. A weighing procedure is going to be carried out on the sample. We were able to determine the amount of water that was absorbed by the sample by doing a computation using the equation that is presented below.



Figure 3.19 Oven used to Dried Specimen

3.6 Mechanical Test

3.6.1 Mechanical (Tensile)

A universal machine was used to perform the tensile testing. The following conditions were used: 5 mm/s displacement. Each formula was tested with three samples (Palacio et al.,2020). ASTM D638 tensile properties were evaluated using a Universal Testing Machine with a crosshead speed of 30mm/min. The dumbbell-shaped specimens were ready for testing after conditioning at room temperature and 30% relative humidity. Figure 3.20 shows the tensile test machine.

The Shimadzu precision universal tester Autograph AG-X plus was employed to assess the tensile properties of various formulations. In order to ensure accuracy and reliability, five replicates of each formulation were meticulously examined. Tensile strength measurements were conducted using Type-1 Dumbbell-shape specimens with dimensions of 165mm x 13mm x 4mm. The tensile tests specifically focused on R-WoPPc with MAPE and adhered

to the standards outlined by ASTM-D638. The tests were conducted at a controlled speed of 5mm/min to ensure consistent and comparable results across all samples. Once the universal tester reached its pre-determined stopping point, the corresponding tensile test data were automatically recorded for further analysis and evaluation. Figure 3.20 shown the tensile test machine. Procedure of tensile test in shows Table 3.9.

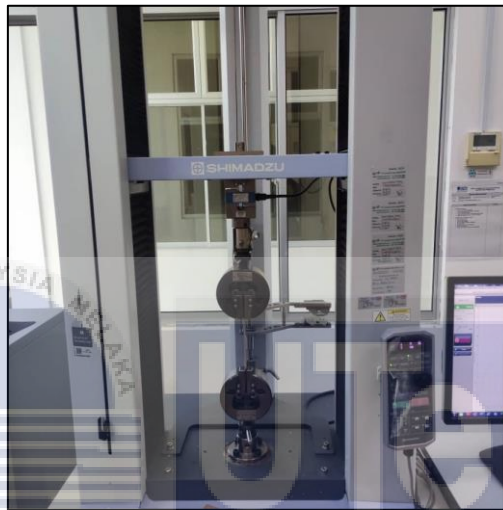


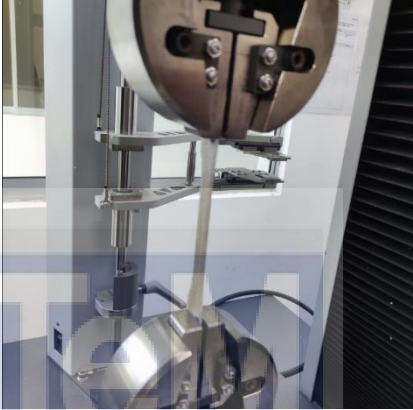
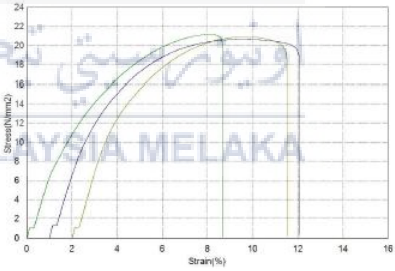


Figure 3.20 Tensile test Machine

UNIVERSITI TEKNIKAL MALAYSIA MELAKA
 اونیورسیتی تکنیکل ملیسیا ملاک
 UNIVERSITI TEKNIKAL MALAYSIA MELAKA

Table 3.9 Procedure Tensile Test

No.	Process	Figure
1.	ASTM-D638 tensile specimen preparation	

2.	Insert the spicemen between the chucks of the tensile machine and tighten the skru.	
3.	Tensile tests on R-WoPPc with MAPE were performed in accordance with ASTM-D638 at a tensile test speed of 5mm/min.	
4.	When the machine stops automatically, the test results will be recorded.	

3.6.2 Mechanical (Flexural)

According to earlier research conducted by Testing et al. (2018), flexure tests, despite their seeming simplicity, have their own unique set of difficulties. The most important factors are

the concentration of compression stress at the central loading point and the fretting wear that occurs at the outside loading points. Wear at the exterior loading sites is especially important when displacement control is performed. This is due to the fact that the required reference points of displacement, which are the tensile face of the specimen, are lost. Figure 3.21 shows the flexural test machine. The procedure for the bending test is outlined in Table 3.10.

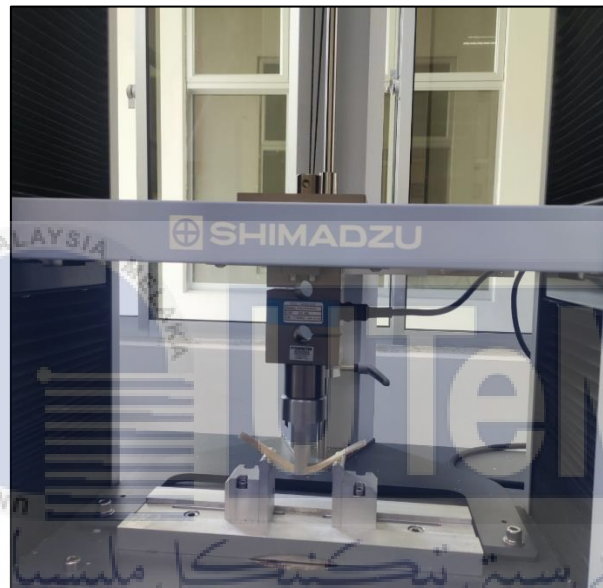

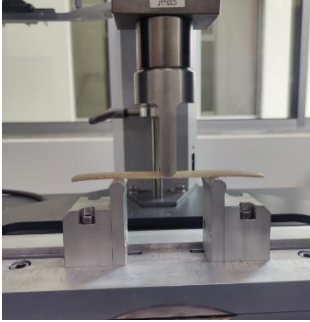
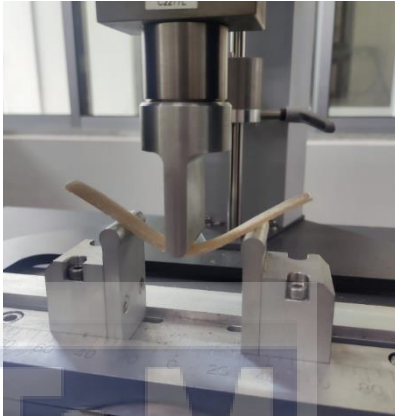
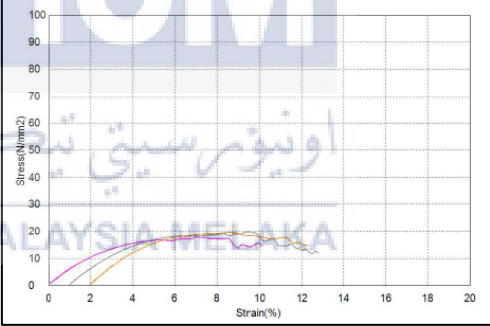


Figure 3.21 Flexural Test Machine

Table 3.10 Procedure Flexural Test

No.	Process	Figure
1.	ASTM D790 tensile specimen preparation	

2.	Insert the spicemen at the middle of mid span.	
3.	Flexural tests on R-WoPPc with MAPE were performed in accordance with ASTM-D790 at a flexural test speed of 2mm/min.	
4.	When the machine stops automatically, the test results will be recorded.	

CHAPTER 4

RESULTS AND DISCUSSION

4.1 Introduction

In this chapter presents the result of effectiveness of MAPE on wood fibre (WF) reinforced recycled polypropylene (rPP) by using mechanical and morphological testing. Different parameters of MAPE was used to determine strength effect of the polymer matrix used which is (rPP). The outcome of the graph was analyzed and discussed for mechanical and morphological testing of the sample. This result is relevant to the intent of this paper.

4.2 3D Printing Filament Produced

4.2.1 Extrusion

The composite of wood fiber, polypropylene and MAPE which has been crushed was mixed and extruded using a Single Extruder at FKM composite lab. For the mixing process, four ratios were used which are 0%, 1%, 3% and 5% of MAPE loading, respectively. The temperature profile was set to 180°C this included the temperature of the barrel and the nozzle. The temperature was chosen based on the melting point of the PP. The speed of the screw was set to 200 rpm and the traction speed set to 16 – 20 rpm due to maintain the filament size in the range of 1.6 – 1.85 mm which is the ideal size to set up to the 3D printing process. For the extrusion process filament 1% MAPE loading which is the first attempt of extrusion process going smoothly in the beginning process but somehow after 3 hours process the filament was a little bit sticky at the entry of cooling bath which is the small hole that filament need to flow as shown in Figure 4.1 and Figure 4.2 shown the sample of sticky filament. So,

the solution water bath was removed then the process went smooth again. For the rest of the MAPE loading filament extrusion process going smooth with the ideal range of filament size. The result shows filament with percent of 1%MAPE has a smooth surface and much better than 0% of MAPE. In addition to enhancing the wettability and plasticization of the WF, the inclusion of MAPE has the potential to improve the interfacial connection between the WF and the matrix, thereby protecting the WF from damage that may occur during the reprocessing process(Zhou et al., 2022). Figure 4.3 shows the printing filament. Figure 4.4 shows the Filament & Microscope image of 0% MAPE, Figure 4.5 shows Filament & Microscope image of 1% MAPE, Figure 4.6 shows Filament & Microscope image of 3% MAPE and Figure 4.7 shows Filament & Microscope image of 5% MAPE.



Figure 4.1 Entry hole of Cooling Bath



Figure 4.2 Sample filament sticky at entry hole cooling bath

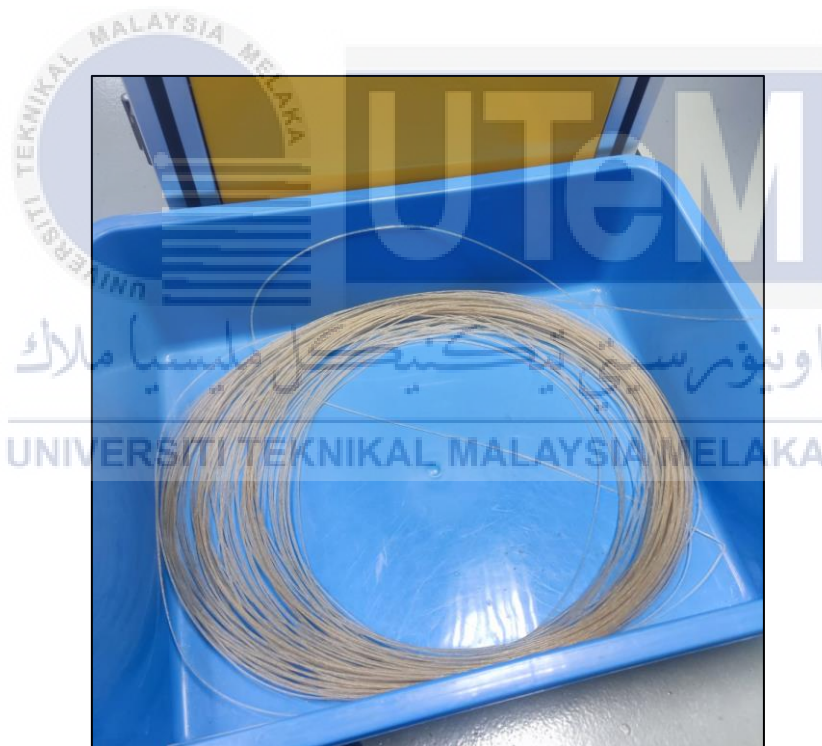


Figure 4.3 Printing Filament



Figure 4.4 Filament & Microscope image of 0% MAPE



Figure 4.5 Filament & Microscope image of 1% MAPE



Figure 4.6 Filament & Microscope image of 3% MAPE



Figure 4.7 Filament & Microscope image of 5% MAPE

4.3 3D Printing Sample

4.3.1 3D Printing

After the filaments were extruded, it was cut to lengths of 3000mm and 2500mm. Each filament was divided into three samples, three 3000mm filaments for tensile testing and three 2500mm filaments for flexural testing. The following MAPE percentages were determined using two types of specimens: 0%, 1%, 3%, and 5%. The tensile test specimen structure was (Type 1, ASTM D638), which is a dog bone structure with dimensions of 165 x 19 x 3mm. And the ASTM D790 structure was employed for the flexural test specimen, with dimensions of 127 x 13 x 3mm. Each structure is created in Solidworks 2019 programme, and the file saved as a .stl file to be open in Ultimaker Cura software for parameter set up. After setting up the parameter, the tensile specimen took 56 minutes to print while the flexural specimen took 38 minutes to print.

Before beginning print, the specimen's parameter was set for all MAPE percentages. The starting settings for the parameters employed in the printing process are 220°C for the nozzle and 85°C for the bed. Before beginning, the nozzle was pre-heated at 220°C to guarantee that the filament flowed out and did not become trapped. The bed was so hot at that parameter

setting that the hotbed painter tape self-absorbed. Because of this issue, specimens curled throughout the printing process as shown in Figure 4.8. During that period, the action taken is to double the layer of tape and to tape cover the brim of the printed specimens. After a few parameter changes, the best parameter for producing specimens that are not curved was discovered to be 197°C for the nozzle temperature and 70°C for the bed temperature. However, in that case, the printing occurred over the weekend, and the air conditioning was turned off. As a result, the specimens generated are flawless. The air conditioning was turned on during the weekday printed. That influenced the specimen quality, but it was better than the previous parameter. The specimens produced were slightly bent, but far better than before the parameter was changed. Figure 4.9 shows the type of specimen which has been produced.



Figure 4.8 Specimen Bent



Figure 4.9 Type of Specimen

4.4 Physical Properties

4.4.1 Water Absorption

Due to the connection of hydrophilic groups of WFs with water, the water absorption behavior of r-WoPPc with MAPE demonstrated a significant effect on durability. The water absorption rate (WAR) of all the filaments substantially increased upon increasing the MAPE content, as shown in Table 4.1. This was a result of increasing the MAPE content. When compared to the other composite samples, which had WAR values of 1.75%, the composites that contained 5% MAPE displayed much lower WAR values. The reason for the decrease in water absorption of the compatible r-WoPPc filament was due to the fact that

MAPE increased the interfacial adhesion between the WF and the matrix. Through the addition of MAPE, the polymer matrix may be able to encapsulate a greater number of WFs and prevent water from penetrating between the WF-matrix interface. Moreover, the water absorption had a significant reduction once the MAPE level was increased even further to 5% working fluids. The presence of 5% MAPE served as a compatibilizer, which resulted in an improvement in the adhesion between the surfaces. Through the application of a 5% loading of MAPE toward R-WoPPc, the water absorption rate is reduced, which results in an improvement in the mechanical characteristics. A higher MAPE content with better flowability could consume many more hydroxyl groups on the WFs surface, which allowed it to wet WFs more efficiently (Zhou et al., 2022).

Table 4.1 Result of the water absorption for R-WoPPc with different loading MAPE

Content MAPE (%)	Initial Weight (g)	Weight after immerge (g)	Total Water Absorb (g)	Water absorption(%)
0%	0.049	0.054	0.005	9.26
1%	0.054	0.055	0.002	3.45
3%	0.050	0.052	0.002	3.45
5%	0.056	0.057	0.001	1.75

When it comes to determining the applications of composites, the water absorption of R-WoPPc composites produced with MAPE is a crucial factor to consider. The results of water absorption for R-WoPPc compounds at various MAPE loadings are depicted in Figure 4.10. The increase in MAPE loading was accompanied by an increase in the amount of water that was absorbed. It was discovered that the water absorption of 0% MAPE results in the highest value, which is 9.26%. The WAR between 0% and 1% show the big different wit 9.26% and 3.45%. Adding MAPE could help polymer matrix encapsulate more WFs and prevent the water penetrate between the WF-matrix interface (Zhou et al., 2022). There is no difference

in the value of water absorption between 1% and 3%, which results in the same value of 3.45% for both percent of MAPE value. It is possible to determine the presence of voids by comparing the absorption weight of R-WoPPc with that of MAPE. A visual representation of the impacts of MAPE loading on the void situation of R-WoPPc value can be found in Figure 4.6.

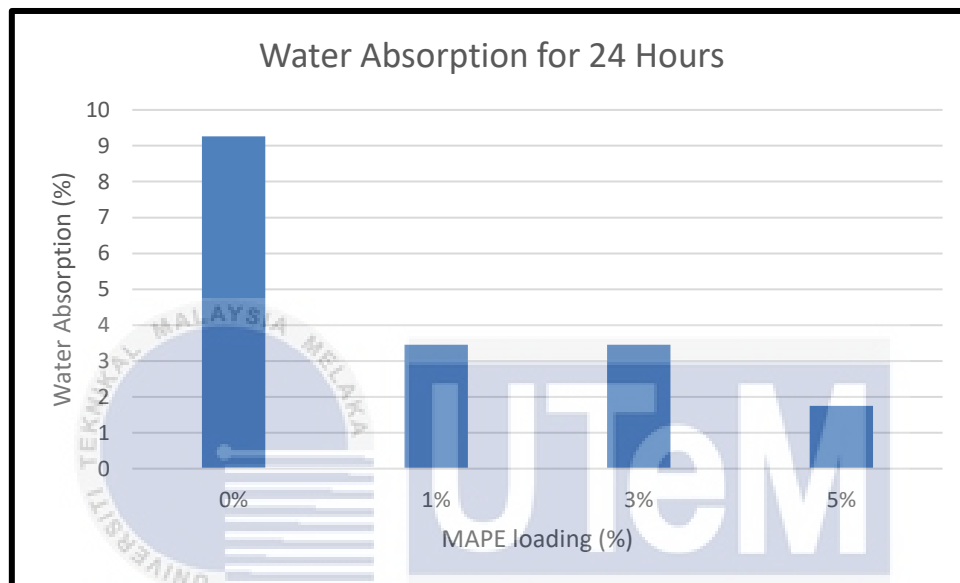


Figure 4.10 Water Absorption for 24 Hours

4.5 Mechanical Properties

4.5.1 Tensile Test

Tensile strength is a mechanical property that is particularly important and dominant in the design and manufacturing processes of buildings. Each material or ingredient has unique features. A test is required to determine the mechanical properties of a material, and one of the most commonly used tests is the tensile test. This test determines the strength level of a material as well as recognises the material's properties. In this test the result were appeared the graph of stress (N/mm^2) vs strain (%). Three specimens of each MAPE loading were tested using SHIMADZU universal tensile testing machine at. A tensile test was perform for

all three sample of four different percent of MAPE loading (0%, 1%, 3%, and 5%). And the speed used was 5mm/min.

For the 0% MAPE loading, specimen 1 has the highest tensile strength of 15.1325 N/mm². However, there are two further specimens with values that are very near to each other: 12.8796 N/mm² for specimen 2 and 13.3102 N/mm² for specimen 3. The value difference between the two specimens is 0.4306 N/mm². The average of these three specimens is given as 13.7741 N/mm². Figure 4.11 shows the tensile strength of 0% MAPE loading.

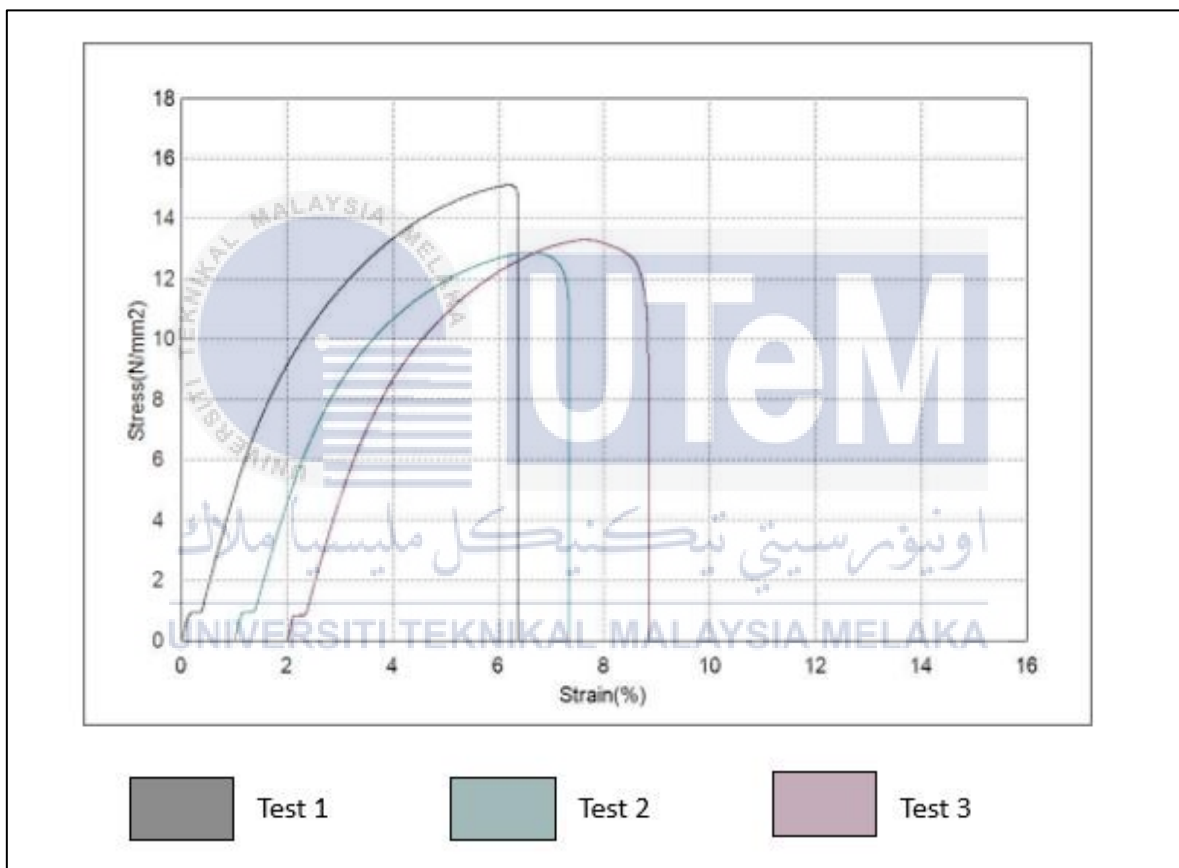


Figure 4.11 Tensile Strength of 0% MAPE loading

For 1% of MAPE loading, the highest value of tensile strength is specimen 3 which is 19.6473 N/mm². Then follow by the specimen 1 with the value is 16.9286 N/mm². for the lowest value of tensile strength is specimen 2 with 15.1063 N/mm². This three specimens have the significant different values gap from each other. This could be owing to the

curvature caused by the printing process, This could be owing to the curvature caused by the printing process, which would negatively impact the tensile strength result of 1% loading MAPE. The average of 3 specimens value was taken which is 16.8941 N/mm² to be compared to other % MAPE loding result. This could be the best solution to determine the tensile strength of this 1% of MAPE loading. Figure 4.12 shows the result of tensile strength of 1% MAPE loading.

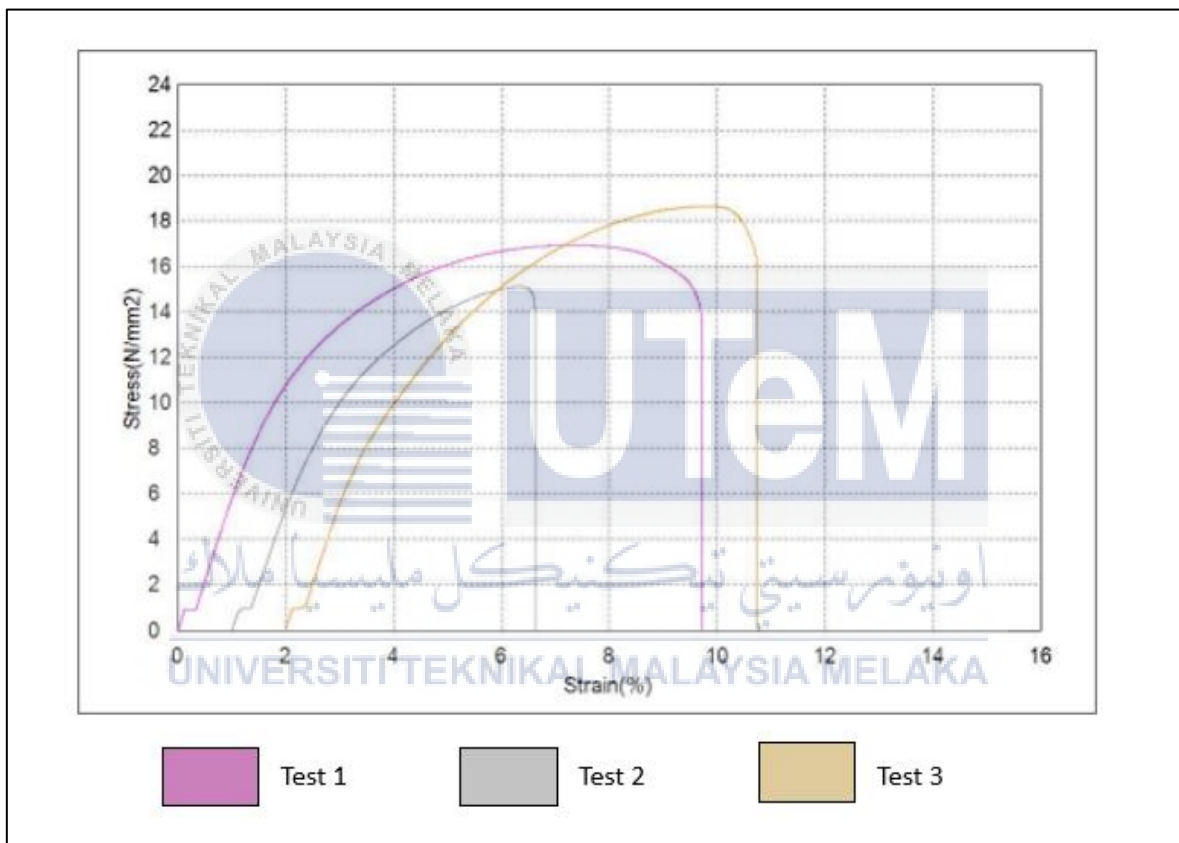


Figure 4.12 Tensile Strength of 1% MAPE loading

For 3% of MAPE loading,specimen 1 shows the highest value of tensile strength which 18.8312 N/mm². The followed by specimen 3 by 17.2219 N/mm² and the lowest value is specimen 2 with 16.8562 N/mm². In this case, one of the specimen does not fully break which is specimen 2. The result of the specimen 2 shown in Figure 4.13 there was the only

one different reading from the others. Based on this three values, the average can be calculated which is 17.6364 N/mm^2 .

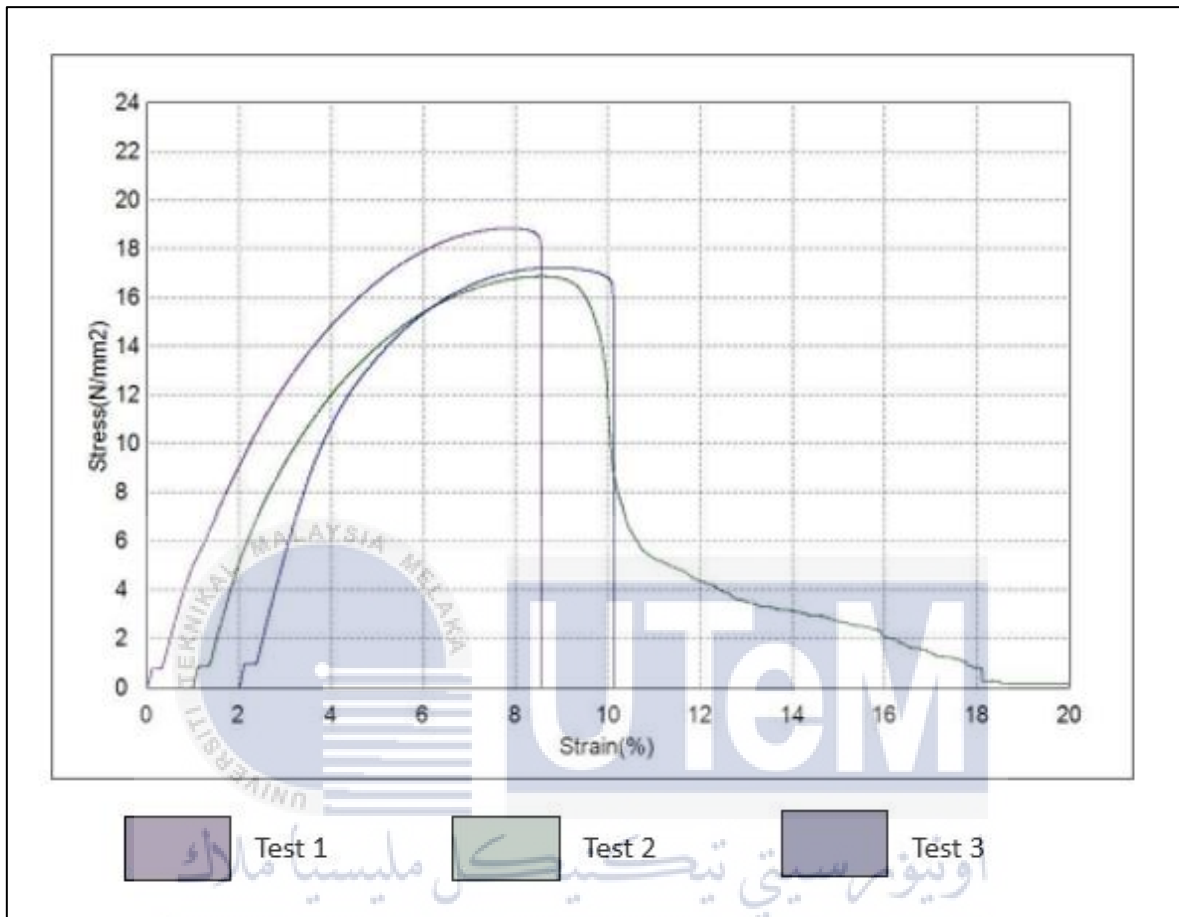


Figure 4.13 Tensile Strength of 3% MAPE loading

For 5% MAPE loading, specimen 1 has the highest tensile strength value of the three other specimens. Specimen 1 has a value of 21.1564 N/mm^2 . The tensile strength value for the second specimen is 20.6220 N/mm^2 , which is the lowest of the three specimens. The third specimen was tested, and the result was 20.8818 N/mm^2 . The tensile strength value of 0% MAPE loading is nearly exact since three distinct samples have values that are quite similar to each other. The average value of tensile strength of 5% MAPE loading is 20.8867 N/mm^2 . Figure 4.14 shows the result of tensile strength of 5% MAPE loading.

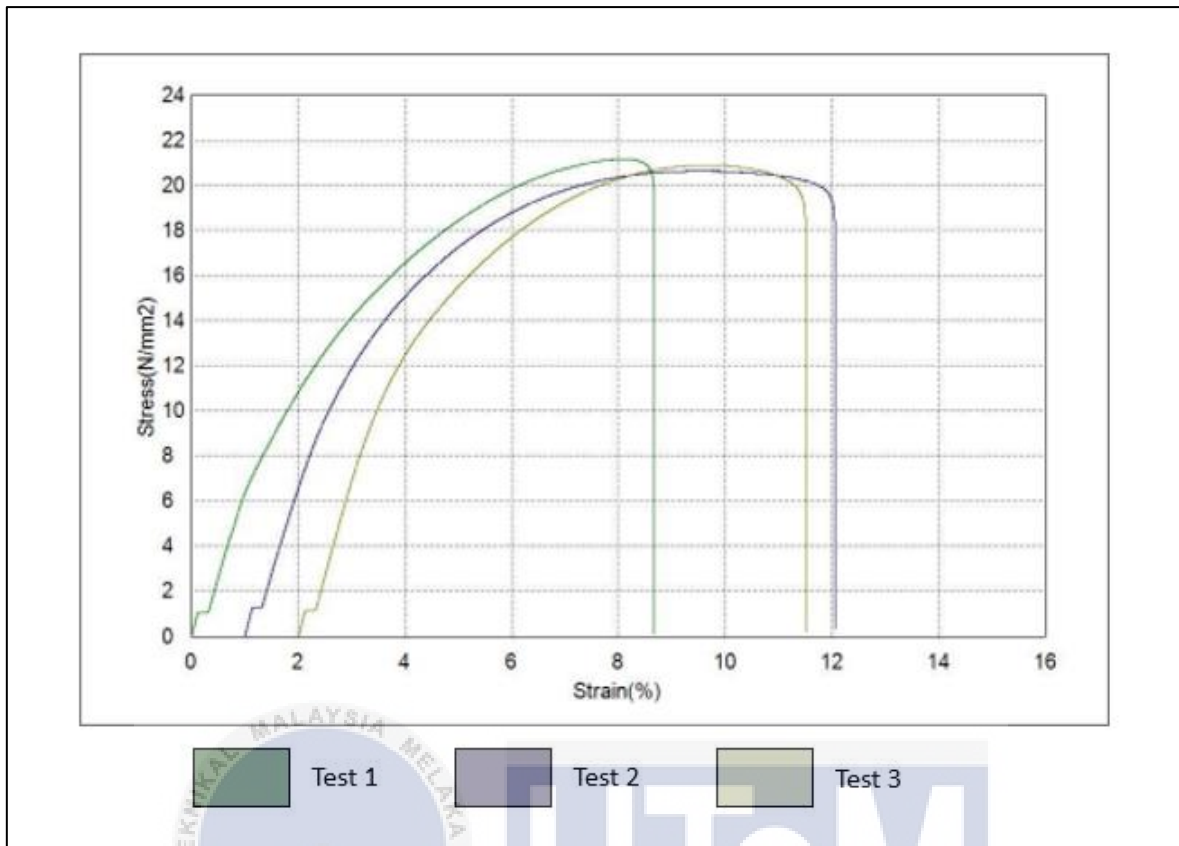


Figure 4.14 Tensile Strength of 5% MAPE loading

In regard to the fact that the mechanical characteristics of MAPE varied depending on the loading, the R-WoPPc with MAPE was explored as a benchmark. In accordance with the data presented in Figure 4.15, the tensile characteristics of polymer matrices experienced a small improvement after being mixed with 1% MAPE. First and foremost, the incorporation of MAPE into the r-WoPPc was done with the intention of enhancing its mechanical qualities. The addition of MAPE was to improve the mechanical properties in the r-WoPPc were the main cause of this research.

The graph of tensile strength is displayed in Figure 4.15. Table 4.2 displays the effect of MAPE as a compatibilizer for r-WoPPC on their tensile strength and modulus elasticity. Figure 4.16 also displays the graph of modulus elasticity. The general trend in tensile strength has been observed to be increasing as the loading MAPE has been increasing according to rising loading. Tensile strength was rises from 13.7741 at 0% to 20.8867 at 5%.

It clearly revealed that by the introduction of 1% MAPE to the composites, it increases the tensile strength and modulus of elasticity of the polymer composites, and this continues until the MAPE reaches 5%. Following the study of the compatibilizer on the composite that was constructed using recycled PP and recycled WD, it was discovered that the tensile strength of the composite was slightly higher than that of the 0% MAPE. According to figure 4.15, the composite that contains 5% MAPE has a higher tensile strength with a maximum value of 20.8867 N/mm². The composite with 1% MAPE has a tensile strength of 16.8941 N/mm², while the composite with 3% MAPE has a tensile strength of 17.6364 N/mm². The composite with 0% MAPE has a tensile strength of 13.7741 N/mm². Based on the Figure 4.15, this tensile strength result show two increases that are relatively significant, namely from 0% to 1% and from 3% to 5%. When the percentage of MAPE in r-WoPPc is increased from 0% to 1%, it is widely known that this causes the tensile strength of the material to increase. This may be attributed to a specific reaction of r-WoPPc to 5% MAPE loading, as the result was very high when the percentage was increased from 3% to 5%. The integration of malleated resulted in an increase in the tensile strength, making it more effective as a compatibilizer for compounds that were created with 5% of MAPE rather than 1% or 3% of MAPE loading. In conclusion, the addition of the coupling agent MAPE to R-WoPPc at dosages ranging from 1% to 5% will result in an increase in tensile strength. It was determined that a MAPE loading of 5% would result in the best tensile strength. a higher MAPE content within an appropriate range improved the mechanical strengths (Zhou et al., 2022). This was the optimal value. The findings are in agreement with the findings of the study that was conducted by (Hao et al. (2021b)), who found that the insertion of maleate-type coupling agents in compounds made from natural fibers led to an increase in the tensile strength of the material. As the percentage of MAPE loading increases, the tensile strength also increases.

Table 4.2 The average Tensile Strength and Modulus Elasticity

Loading MAPE (%)	Tensile Strength (N/mm ²)	Modulus Elasticity (N/mm ²)
0%	13.7741	236.6013072
1%	16.8941	248.4894215
3%	17.6364	237.0557154
5%	20.8867	258.1482814

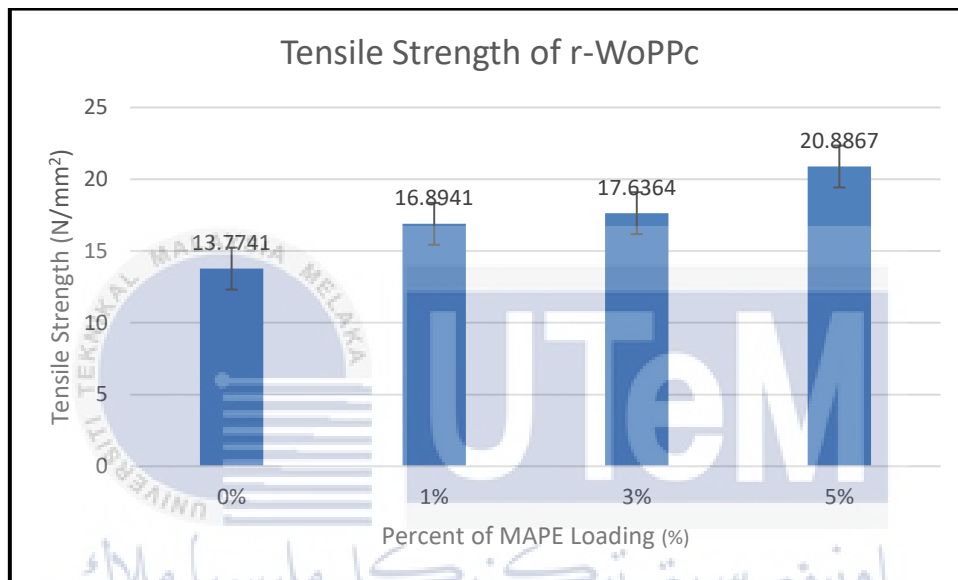


Figure 4.15 Tensile Strength of r-WoPPc

The rPP, WF, and MAPE all contribute to the formation of the Young modulus, also known as the modulus strength, of the rubber compound. Therefore, the coupling agent MAPE was applied during the hot press process in order to strengthen the bonding between the interfaces and to enhance the mechanical properties of the material. As demonstrated in Figure 4.16, the incorporation of MAPE into the composites resulted in a notable enhancement in the Young Modulus Elasticity.

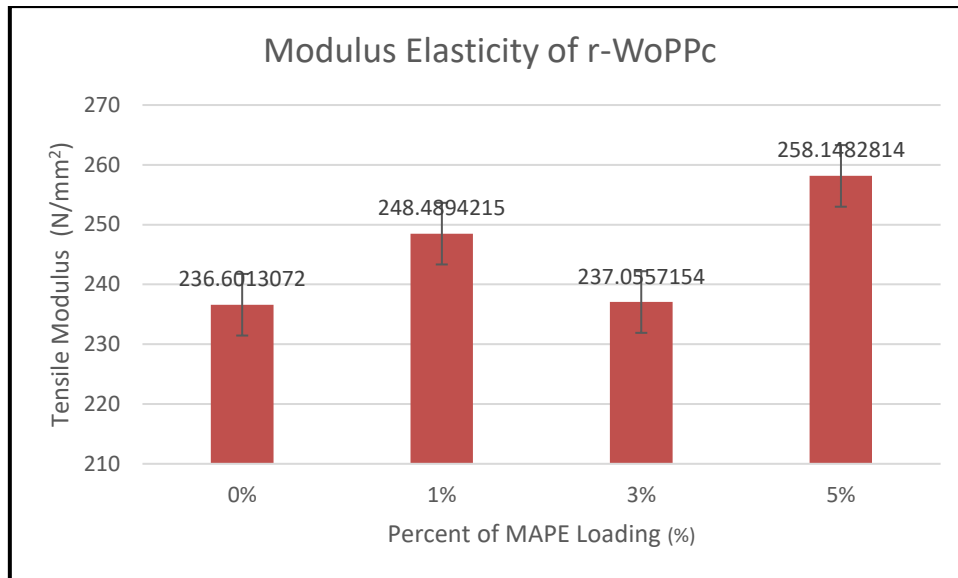


Figure 4.16 Modulus Elasticity of r-WoPPc

The Modulus of Elasticity of the R-WoPPc show the increase in their trend as MAPE loading increase from 236.6013072 N/mm² at 0% to 258.1482814 N/mm² at 5% . As can be shown in Table 4.2, the R-WoPPc with 5% MAPE exhibited a greater Young Modulus of Elasticity, which was measured at 258.1482814 N/mm². But somehow at 3% of MAPE the value of elasticity was suddenly decrease with 237.0557154 N/mm². As a conclusion, it can be stated that an increase in the percentage loading of MAPE is similarly favorable to an increase in the modulus of elasticity(Hao et al., 2021b).

4.5.2 Flexural Test

Flexural test is also a mechanical property that is particularly important and dominant in the design and manufacturing processes of buildings. flexural test is a continuation of tensile test. Each material or ingredient has unique features. A test is required to determine the mechanical properties of a material, and one of the most commonly used tests after tensile is flexural test. This test determines the strength level of a material as well as recognises the material's properties. In this test the result were appeared the graph of stress (N/mm²) vs strain

(%). Three specimens of each MAPE loading were tested using SHIMADZU universal tensile testing machine at FTKIP main campus. A tensile test was performed for all three samples of four different percent of MAPE loading (0%, 1%, 3%, and 5%). And the speed used was 2mm/min.

When subjected to a MAPE loading of 0%, specimen 2 demonstrates the maximum flexural strength, measuring 19.8756 N/mm². In second place was specimen 3, which had a value of 19.6840 N/mm², while specimen 1 had the lowest value, which was 18.1235 N/mm². The value of 19.2277 N/mm² is the average of these three specimens, according to the data. In Figure 4.17, the flexural strength of the material is shown with 0% MAPE loading.

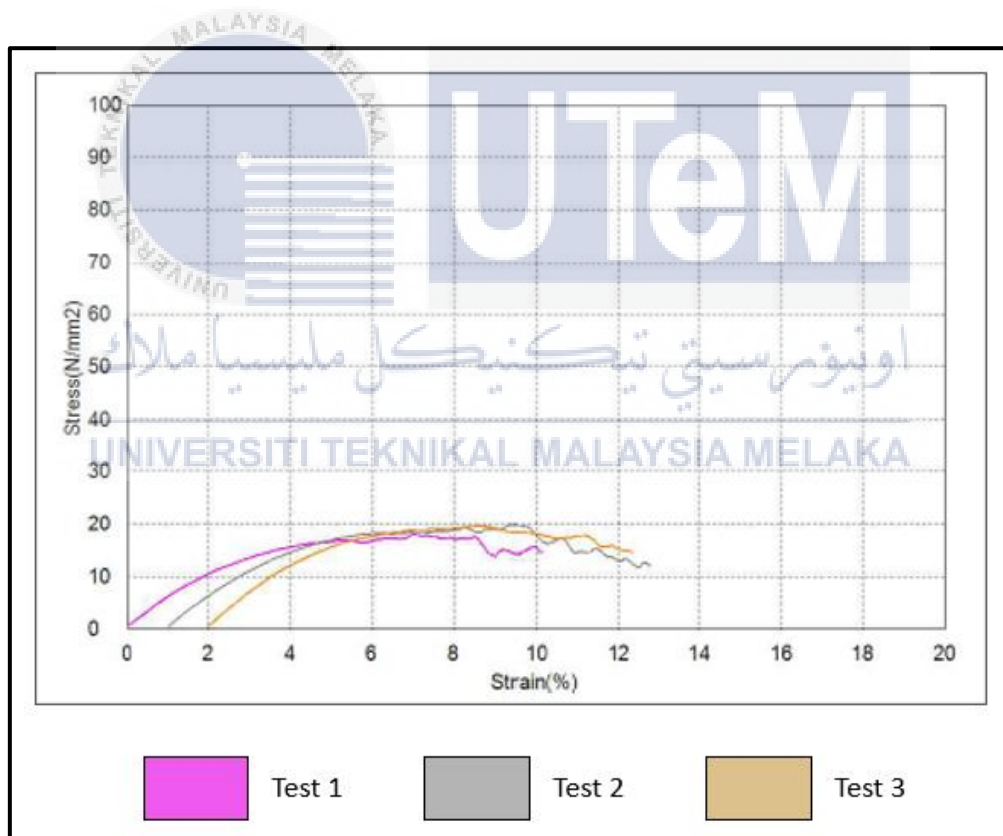


Figure 4.17 Flexural Strength of 0% MAPE loading

The greatest result of flexural strength comes from specimen 1, which has a value of 24.1845 N/mm² when applied to a MAPE loading of 1%. The second specimen, which has a value of 23.6592 N/mm², comes next in the sequence. The specimen 3 has the lowest value of flexural strength, which is 22.7197 N/mm², among all the specimens. These three specimens have a substantial difference in values from one another in comparison to one another. This could be due to the curvature that was generated by the printing process, which would have a negative impact on the flexural strength result of 1% loading MAPE. This could be due to the fact that the printing process caused the curvature. The average value of three specimens was calculated, and it was found to be 23.5211 N/mm². This value was then compared to the other MAPE loading results. The flexural strength of this 1% MAPE loading might be determined using this method, which is possibly the most effective solution. The flexural strength of the material after being loaded with 1% MAPE is depicted in Figure 4.18.

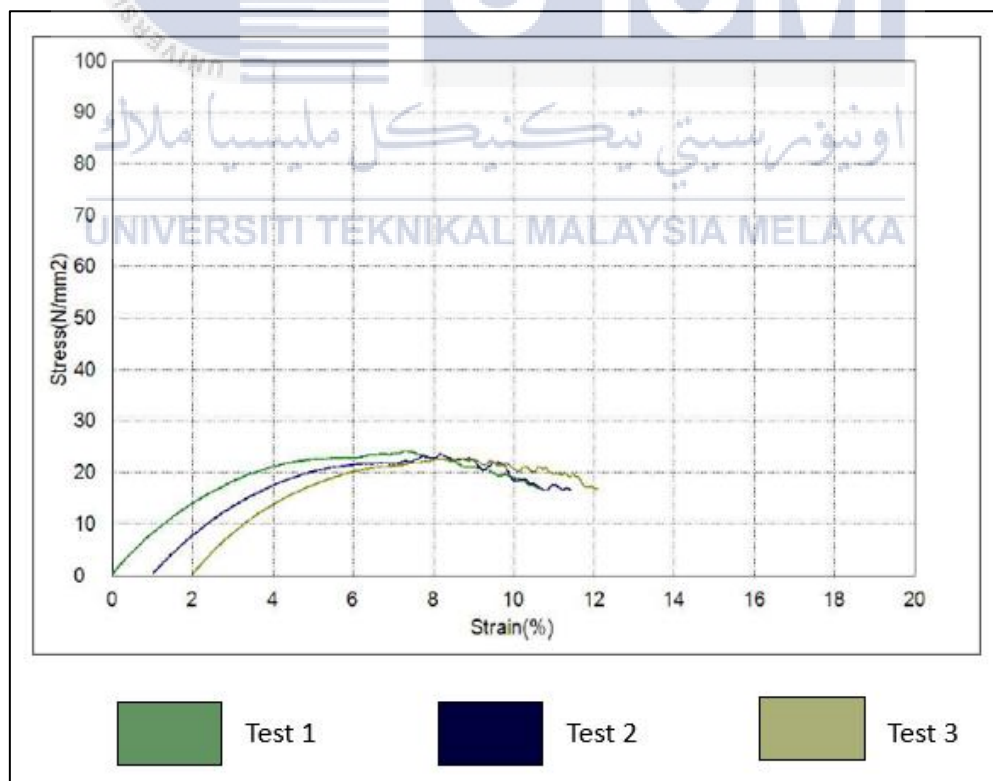


Figure 4.18 Flexural Strength of 1% MAPE loading

Specimen 2 reveals the highest value of flexural strength, which is 23.7989 N/mm², when three percent of the MAPE loading is applied. The specimen with the highest value is specimen 3, which has a value of 21.2032 N/mm², followed by specimen 1 with a value of 22.1090 N/mm². The outcome of the second specimen, which is depicted in Figure 4.19. On the basis of these three numbers, it is possible to determine the average, which comes out to be 22.3704 N/mm².

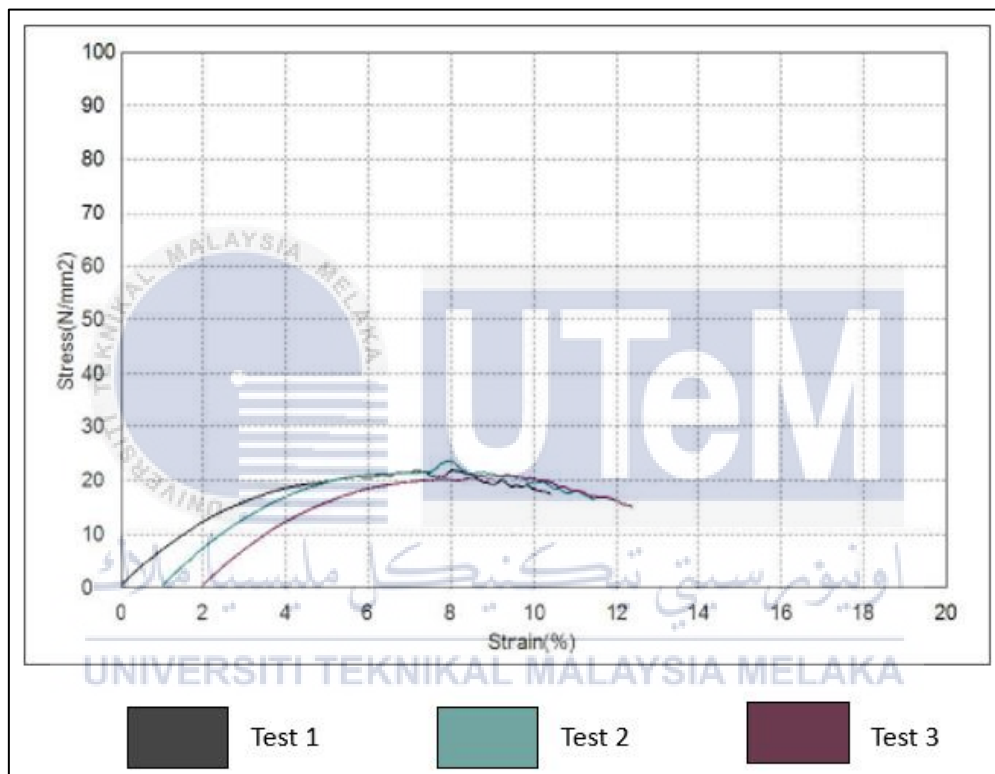


Figure 4.19 Flexural Strength of 3% MAPE loading

In comparison to the other three specimens, specimen 2 exhibits the highest flexural strength value when tested to a MAPE loading of 5%. The strength of specimen 2 is measured at 25.7735 N/mm². The value of the flexural strength for specimen 3 is 22.0262 N/mm², making it the specimen with the lowest value out of the three types of specimens. Following the examination of specimen 1, the result was found to be 23.0898 N/mm². The value of the flexural strength at 0% MAPE loading is really close to being precise due to the fact that three different samples have values that are quite comparable to one another. When subjected to a 5% MAPE loading, the flexural strength of the material is 23.6298 N/mm² on average. The results of the flexural strength test with a 5% MAPE loading are displayed in Figure 4.20.

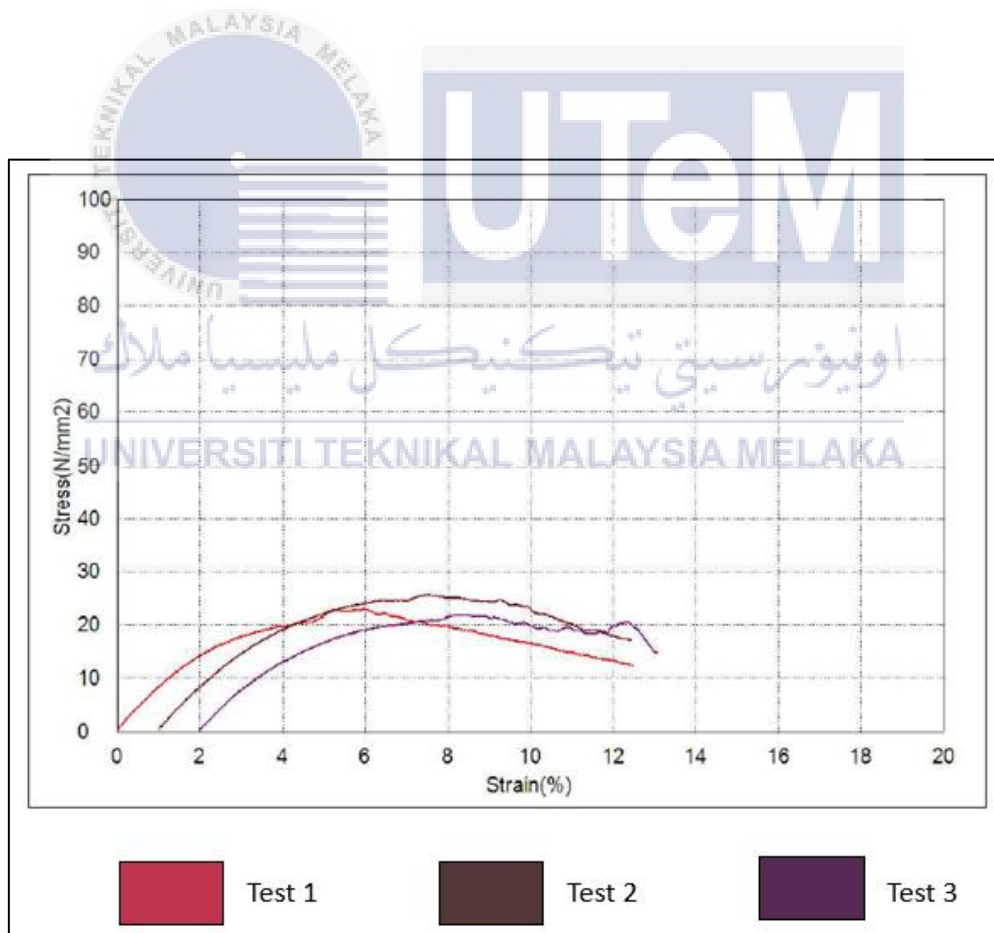


Figure 4.20 Flexural Strength of 5% MAPE loading

The effects of the MAPE contents on the flexural properties of the r-WoPPc are depicted in Figure 4.21 and 4.22, as well as in Table 4.3. Each MAPE loading was evaluated by employing three samples of specimens for each MAPE loading used in the testing. Table 4.3 presents the average values for flexural strength and elasticity for five different samples, each of which was subjected to a different type of loading: 0%, 1%, 3%, and 5% of MAPE. Increasing the trend from 0% to 5%, which is equivalent to 19.2277 N/mm² to 23.6398 N/mm², the flexural strength demonstrates an increase in the trend. For example, the result of flexural strength indicates a significant rise from 19.2277 N/mm² to 23.5211 N/mm² when the percentage is increased from 0% to 1%. According to the findings, the inclusion of MAPE has the potential to enhance the mechanical properties of r-WoPPc (Hao et al., 2021a). The compatibilizer of MAPE was primarily responsible for the observed enhancement in the flexural strength of the R-WoPPc material when it was treated with 1% MAPE. On the other hand, the result for 3% demonstrates a minor reduction from the 1%, which is 22.3704 N/mm², and the result for 5% demonstrates a positive increase with the number 23.6298 N/mm², which is the highest value among the four MAPE loadings. For the purpose of recycling end-of-life WPC goods into high-performance composites, the aforementioned results suggest that the integration of waste WFs and the utilisation of MAPE as a compatibilizer could be a straightforward and inexpensive solution (Zhou et al., 2022).

Table 4.3 The average Flexural Strength and Elasticity

Loading MAPE (%)	Flexural Strength (N/mm ²)	Elasticity (N/mm ²)
0%	19.2277	258.9474138
1%	23.5211	340.334067
3%	22.3704	298.9488201
5%	23.6298	376.8563883

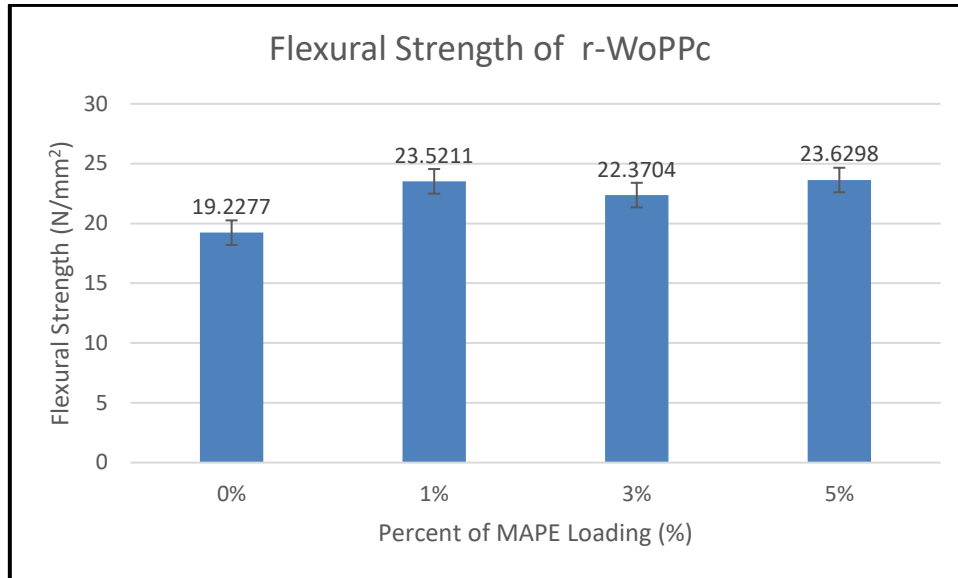


Figure 4.21 Flexural Strength of r-WoPPc

All of the flexural modulus and elasticity values of the MAPE compatibilizer R-WoPPc were found to be greater than those of the R-WoPPc that did not contain the compatibilizer, as demonstrated in figure 4.22. Flexural elasticity grew from 258.9474138 N/mm² for 0% to 376.8563883 N/mm² for 5% over most of the overall course of the trend. There was a significant increase in the value of the flexural strength from 258.9474138 N/mm² to 340.334067 N/mm² when the percentage was increased from 0% to 1%. The fact that this is the case suggests that the improved reinforcing efficiency of r-WoPPc was accomplished by enhancing the r-WoPPc matrix interface with Maleated anhydride grafted polyethylene (MAPE) with only a 1% addition. Despite the fact that the value of elasticity decreased for the 3%, it was still within the acceptable range. There is a possibility that it will cause the specimen to warp throughout the printing process. If this occurs, the 5% will exhibit the greatest value of elasticity, which is 376.8566883 N/mm². Furthermore, the composites that involved MAPE agent coupling and compatibilizer demonstrated comparable flexural strength and elasticity at a concentration of 5% MAPE. Based on the findings presented above, it was determined that the enhancement of the R-WoPPc matrix interface through the

incorporation of MAPE as a compatibilizer or agent coupling was the primary mechanism responsible for the enhancement of the mechanical properties of composites(Zhou et al., 2022).

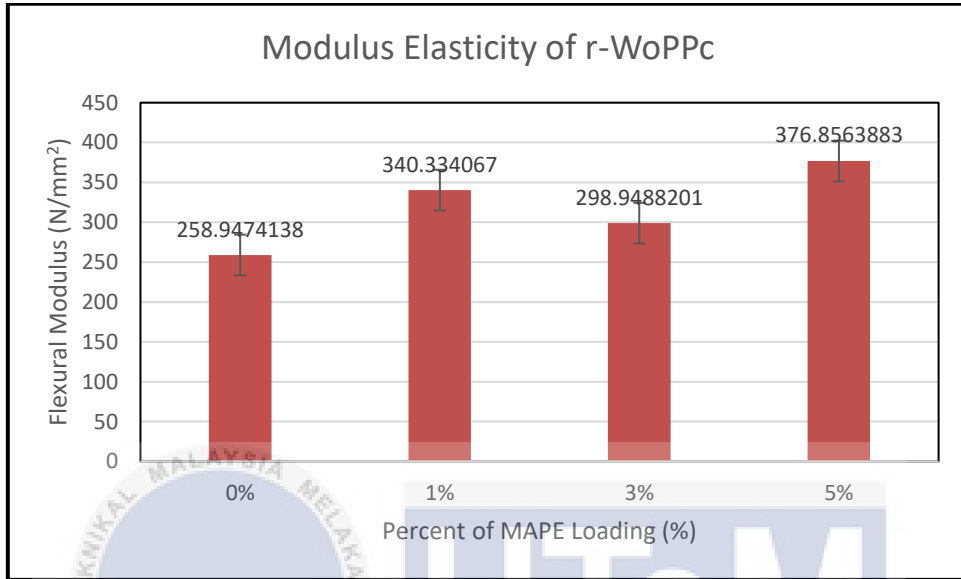


Figure 4.22 Elasticity of r-WoPPc

4.6 Summary

The water absorption testing results show that the water absorption rate (WAR) of all filaments significantly increased with increasing MAPE content. The decrease in water absorption in compatible R-WoPPc was due to increased interfacial adhesion between the WF and matrix. The addition of MAPE allowed the polymer matrix to encapsulate more WFs and prevent water from penetrating the WF-matrix interface. The water absorption of 0% MAPE resulted in the highest value of 9.26%, while 1% and 3% had no difference in water absorption. The presence of voids was determined by comparing the absorption weight of R-WoPPc with that of MAPE. The mechanical properties of r-WoPPC composites showed a significant increase in tensile strength from 0% to 1%, and flexural strength from 0% to 1%. When the MAPE content was increased further, the tensile modulus initially increased

and then stabilised, but the flexural modulus first increased and then fell over the process of raising the MAPE content (Zhou et al., 2022).The addition of MAPE increased the mechanical strength of r-WoPPC.



CHAPTER 5

CONCLUSION AND RECOMMENDATIONS

5.1 Conclusion

The study target of (1) to fabricate a new 3D printer filament from recycle Polypropylene (PP), wood fiber and maleic anhydride polyethylene (MAPE) has been accomplished by the completion of a number of studies. (2) to determine the impact that maleic anhydride polyethylene (MAPE) has on the mechanical properties of the composite material. These parameters include tensile strength, flexural strength, and water absorption of the material. Based on the findings of the entire investigation, the following are some of the most significant conclusions that may be drawn:

- (1) To fabricate a new 3D printer filament from recycle Polypropylene (PP), wood fiber and maleic anhydride polyethylene (MAPE)

The characteristics of WF, rPP, and MAPE were determined by the application of physical and mechanical qualities. In the present investigation, a siever was utilised to acquire a weight fraction (WF) with a particle size of 125 μm . On the other hand, rPP was already accessible in pellet form. After that, the WF was subjected to an alkaline treatment that involved the use of sodium hydroxide (NaOH) in order to enhance its thermal properties and remove any impurities that were present on its surface. rPP and WF were utilised, and treated MAPE was fully combined with them before being heated using a hot press method. This was done in order to make a pallet that had varying amounts of MAPE loading. Both the r-WoPPc and the MAPE pallet form were subjected to the extrusion process, and the r-WoPPC

filament was manufactured by utilising the parameter setting. In a nutshell, the surface of the 1% MAPE filament is smoother than the surface of the other filament, and there are no voids identified on it. This occurs as a consequence of a process that the r-WoPPC filaments go through, which enables the fibres and polymers to develop a strong link with one another. When sodium hydroxide is used at the beginning of this process, the filaments that are bound together are far more robust than the filaments that were not treated. In addition to this, it provides the fibre and polymer with a higher ability to integrate with the surface. In addition, the water absorption was evaluated for each and every filament that was manufactured, and the findings revealed that 5% of MAPE loading had a lower water absorption rate of 1.75 percent. Furthermore, after the MAPE level was increased even further to 5% working fluids, there was a statistically significant decrease in the amount of water that was absorbed. An increase in the adhesion between the surfaces was brought about as a result of the presence of 5% MAPE, which acted as a compatibilizer. The reduction in the water absorption rate that occurs as a consequence of the application of a 5% loading of MAPE towards R-WoPPC leads to an improvement in the mechanical qualities of the material.

- (2) To determine the impact that maleic anhydride polyethylene (MAPE) has on the mechanical properties of the composite material. These parameters include tensile strength, flexural strength, and water absorption of the material.

This study's goal of assessing the strength on different percent of MAPE loading on the mechanical properties of 3D printed r-WoPPC specimens was successfully achieved. Tensile and flexural tests were used to analyse the mechanical characteristics of r-WoPPC. The same machine measurement was used for testing tensile and flexural strength. In comparison to percent of MAPE, it the 5% of MAPE has highest result of tensile strength and flexural strength, which are 20.8867 N/mm² and 23.6298 N/mm², respectively. But 1% has a

significant result because the value of both tensile and flexural strength has a drastic increment from 0% to 1%. So the 1% shows the good response of the reaction with r-WoPPc composite.

5.2 Recommendations

Further work that can be explored in this study is to investigate the effect of MAPE as a compatibilizer for wood dust fiber and any type of polymer. This is something that can be done in the future. As an example, PLA or ABS. An additional investigation involves adjusting the loading of wood to 5%. Additionally, the filaments can be investigated with regard to their qualities by the use of techniques such as the wire pull test, thermogravimetric analysis (TGA), Fourier transform infrared spectroscopy (FTIR), and differential scanning calorimetry (DSC). Another aspect that could be investigated with regard to this composite is the possibility of substituting the type of wood dust with another fiber, such as coconut fiber. The fiber composition ought to be taken into consideration in terms of its maximum fiber composition in the kind of chemical treatment, such as the chemical treatment with NaOH and the chemical treatment with silane and NaOH. In addition, the preparation of the composite may be studied by utilizing an internal mixer, and the preparation of the filament is being produced by utilizing a twin screw extruder. The composite material that contains MAPE as a compatibilizer can have its mechanical and physical properties improved as a result of this. It is recommended that the specimen be examined using a scanning electron microscope (SEM) machine in order to conduct a comprehensive examination of the specimen.

5.3 Project Potential

There is a significant possibility that the findings of this study could be utilized in the manufacturing sector as a commercial bio composite filament by the industry. Additionally, this filament has the ability to be utilized in any different kind of FDM 3D printing machine, and its pellet can be extruded using any kind of extruder.



REFERENCES

- Abegunde, S. M., Idowu, K. S., Adejuwon, O. M., & Adeyemi-Adejolu, T. (2020). A review on the influence of chemical modification on the performance of adsorbents. *Resources, Environment and Sustainability*, *1*, 100001. <https://doi.org/10.1016/J.RESENV.2020.100001>
- Bao, F. C., Jiang, Z. H., Jiang, X. M., Lu, X. X., Luo, X. Q., & Zhang, S. Y. (2001). Differences in wood properties between juvenile wood and mature wood in 10 species grown in China. *Wood Science and Technology*, *35*(4). <https://doi.org/10.1007/s002260100099>
- Bengtsson, M., Stark, N. M., & Oksman, K. (2007). Durability and mechanical properties of silane cross-linked wood thermoplastic composites. *Composites Science and Technology*, *67*(13), 2728–2738. <https://doi.org/10.1016/J.COMPSCITECH.2007.02.006>
- Carus, M., Gahle, C., & Korte, H. (2008). Market and future trends for wood–polymer composites in Europe: the example of Germany. *Wood-Polymer Composites*, 300–330. <https://doi.org/10.1533/9781845694579.300>
- Crespell, P. J. A. (2008). *Market and technology trends and challenges for wood plastic composites in North America*. https://www.academia.edu/78003927/Market_and_technology_trends_and_challenges_for_wood_plastic_composites_in_North_America
- Dankar, I., Pujolà, M., El Omar, F., Sepulcre, F., & Haddarah, A. (2018). Impact of Mechanical and Microstructural Properties of Potato Puree-Food Additive Complexes on Extrusion-Based 3D Printing. *Food and Bioprocess Technology*, *11*(11). <https://doi.org/10.1007/s11947-018-2159-5>
- Dilberoglu, U. M., Gharehpapagh, B., Yaman, U., & Dolen, M. (2017). The Role of Additive Manufacturing in the Era of Industry 4.0. *Procedia Manufacturing*, *11*. <https://doi.org/10.1016/j.promfg.2017.07.148>
- Ernst & Young. (2016). Identify the impact on business and unlock the 3D printing potential. In *Ernst & Young GmbH*.
- Faruk, O., Bledzki, A. K., Fink, H. P., & Sain, M. (2012). Biocomposites reinforced with natural fibers: 2000–2010. *Progress in Polymer Science*, *37*(11), 1552–1596. <https://doi.org/10.1016/J.PROGPOLYMSCI.2012.04.003>
- Foo, C. Y., Lim, H. N., Mahdi, M. A., Wahid, M. H., & Huang, N. M. (2018). Three-Dimensional Printed Electrode and Its Novel Applications in Electronic Devices. *Scientific Reports*, *8*(1). <https://doi.org/10.1038/s41598-018-25861-3>
- Fu, H., Dun, M., Wang, H., Wang, W., & Wang, Q. (2021). Rheological behavior, internal stress and structural changes of ultra-high-filled wood-flour/high-density polyethylene composite in shear flow field. *Journal of Materials Research and Technology*, *14*. <https://doi.org/10.1016/j.jmrt.2021.07.024>
- Garcia, J., Yang, Z. L., Mongrain, R., Leask, R. L., & Lachapelle, K. (2018). 3D printing materials and their use in medical education: A review of current technology and trends for the future. In *BMJ Simulation and Technology Enhanced Learning* (Vol. 4, Issue 1). <https://doi.org/10.1136/bmjstel-2017-000234>
- Gülcan, O., Günaydın, K., & Tamer, A. (2021). The state of the art of material jetting—a critical review. In *Polymers* (Vol. 13, Issue 16). <https://doi.org/10.3390/polym13162829>

- Hao, X., Xu, J., Zhou, H., Tang, W., Li, W., Wang, Q., & Ou, R. (2021a). Interfacial adhesion mechanisms of ultra-highly filled wood fiber/polyethylene composites using maleic anhydride grafted polyethylene as a compatibilizer. *Materials & Design*, *212*, 110182. <https://doi.org/10.1016/J.MATDES.2021.110182>
- Hao, X., Xu, J., Zhou, H., Tang, W., Li, W., Wang, Q., & Ou, R. (2021b). Interfacial adhesion mechanisms of ultra-highly filled wood fiber/polyethylene composites using maleic anhydride grafted polyethylene as a compatibilizer. *Materials & Design*, *212*, 110182. <https://doi.org/10.1016/J.MATDES.2021.110182>
- Jakob, M., Mahendran, A. R., Gindl-Altmatter, W., Bliem, P., Konnerth, J., Müller, U., & Veigel, S. (2022). The strength and stiffness of oriented wood and cellulose-fibre materials: A review. *Progress in Materials Science*, *125*, 100916. <https://doi.org/10.1016/J.PMATSCI.2021.100916>
- Kazayawoko, M., Balatinecz, J. J., & Matuana, L. M. (1999). Surface modification and adhesion mechanisms in woodfiber-polypropylene composites. *Journal of Materials Science*, *34*(24), 6189–6199. <https://doi.org/10.1023/A:1004790409158/METRICS>
- Keener, T. J., Stuart, R. K., & Brown, T. K. (2004). Maleated coupling agents for natural fibre composites. *Composites Part A: Applied Science and Manufacturing*, *35*(3), 357–362. <https://doi.org/10.1016/J.COMPOSITESA.2003.09.014>
- Khalid, M. Y., Imran, R., Arif, Z. U., Akram, N., Arshad, H., Rashid, A. Al, & Márquez, F. P. G. (2021). Developments in Chemical Treatments, Manufacturing Techniques and Potential Applications of Natural-Fibers-Based Biodegradable Composites. *Coatings 2021, Vol. 11, Page 293, 11*(3), 293. <https://doi.org/10.3390/COATINGS11030293>
- Khalil, H. P. S. A., Rozman, H. D., Ismail, H., & Ahmad, M. N. (2002). Polypropylene (PP)- Acacia mangium composites: The effect of acetylation on mechanical and water absorption properties. *Polymer - Plastics Technology and Engineering*, *41*(3). <https://doi.org/10.1081/PPT-120004362>
- Kristiawan, R. B., Imaduddin, F., Ariawan, D., Ubaidillah, & Arifin, Z. (2021). A review on the fused deposition modeling (FDM) 3D printing: Filament processing, materials, and printing parameters. In *Open Engineering* (Vol. 11, Issue 1, pp. 639–649). De Gruyter Open Ltd. <https://doi.org/10.1515/eng-2021-0063>
- Kristiawan, R. B., Rusdyanto, B., Imaduddin, F., & Ariawan, D. (2022). Glass powder additive on recycled polypropylene filaments: A sustainable material in 3d printing. *Polymers*, *14*(1). <https://doi.org/10.3390/polym14010005>
- Kumar, R., Kumar, K., & Bhowmik, S. (2018). Mechanical characterization and quantification of tensile, fracture and viscoelastic characteristics of wood filler reinforced epoxy composite. *Wood Science and Technology*, *52*(3). <https://doi.org/10.1007/s00226-018-0995-0>
- Lee, J., Kim, H. C., Choi, J. W., & Lee, I. H. (2017). A review on 3D printed smart devices for 4D printing. In *International Journal of Precision Engineering and Manufacturing - Green Technology* (Vol. 4, Issue 3). <https://doi.org/10.1007/s40684-017-0042-x>
- Lee, J. Y., An, J., & Chua, C. K. (2017). Fundamentals and applications of 3D printing for novel materials. In *Applied Materials Today* (Vol. 7). <https://doi.org/10.1016/j.apmt.2017.02.004>
- Liu, L., Meng, Y., Dai, X., Chen, K., & Zhu, Y. (2019). 3D Printing Complex Egg White Protein Objects: Properties and Optimization. *Food and Bioprocess Technology*, *12*(2). <https://doi.org/10.1007/s11947-018-2209-z>
- Liu, Z., Zhang, M., Bhandari, B., & Wang, Y. (2017). 3D printing: Printing precision and application in food sector. In *Trends in Food Science and Technology* (Vol. 69). <https://doi.org/10.1016/j.tifs.2017.08.018>

- Low, Z. X., Chua, Y. T., Ray, B. M., Mattia, D., Metcalfe, I. S., & Patterson, D. A. (2017). Perspective on 3D printing of separation membranes and comparison to related unconventional fabrication techniques. In *Journal of Membrane Science* (Vol. 523). <https://doi.org/10.1016/j.memsci.2016.10.006>
- Marra, A. A. (1992). *Technology of wood bonding : principles in practice / Alan A. Marra.* xvi, 454 p. :
- Martín-Alfonso, J. E., Valencia, C., & Franco, J. M. (2013). Effect of amorphous/recycled polypropylene ratio on thermo-mechanical properties of blends for lubricant applications. *Polymer Testing*, 32(3), 516–524. <https://doi.org/10.1016/j.polymertesting.2013.01.010>
- Matuana, L. M., & Stark, N. M. (2015). The use of wood fibers as reinforcements in composites. *Biofiber Reinforcements in Composite Materials*, 648–688. <https://doi.org/10.1533/9781782421276.5.648>
- Momanyi, J., Herzog, M., & Muchiri, P. (2019). Analysis of thermomechanical properties of selected class of recycled thermoplastic materials based on their applications. *Recycling*, 4(3). <https://doi.org/10.3390/recycling4030033>
- Morales, M. A., Atencio Martinez, C. L., Maranon, A., Hernandez, C., Michaud, V., & Porras, A. (2021). Development and characterization of rice husk and recycled polypropylene composite filaments for 3d printing. *Polymers*, 13(7). <https://doi.org/10.3390/polym13071067>
- Morsing, N. (1998). *The influence of hygrothermal treatment on compression of beech perpendicular to the grain.*
- Nadlene, R., Sapuan, S. M., Jawaid, M., Ishak, M. R., & Yusriah, L. (2018). The effects of chemical treatment on the structural and thermal, physical, and mechanical and morphological properties of roselle fiber-reinforced vinyl ester composites. *Polymer Composites*, 39(1). <https://doi.org/10.1002/pc.23927>
- Nasereddin, J. M., Wellner, N., Alhijaj, M., Belton, P., & Qi, S. (2018). Development of a Simple Mechanical Screening Method for Predicting the Feedability of a Pharmaceutical FDM 3D Printing Filament. *Pharmaceutical Research*, 35(8). <https://doi.org/10.1007/s11095-018-2432-3>
- Olsson, A., Oscarsson, J., Serrano, E., Källsner, B., Johansson, M., & Enquist, B. (2013). Prediction of timber bending strength and in-member cross-sectional stiffness variation on the basis of local wood fibre orientation. *European Journal of Wood and Wood Products*, 71(3). <https://doi.org/10.1007/s00107-013-0684-5>
- Polline, M., Mutua, J. M., Mbuya, T. O., & Ernest, K. (2021). Recipe Development and Mechanical Characterization of Carbon Fibre Reinforced Recycled Polypropylene 3D Printing Filament. *Open Journal of Composite Materials*, 11(03). <https://doi.org/10.4236/ojcm.2021.113005>
- Rahayu, I., Zainuddin, A., Malik, Y. T., & Hendrana, S. (2020). Maleic anhydride grafted onto high density polyethylene with an enhanced grafting degree via monomer microencapsulation. *Heliyon*, 6(4). <https://doi.org/10.1016/j.heliyon.2020.e03742>
- Saad, F. U. S. M., Salim, N., & Roslan, R. (2022). Physical and mechanical properties of kenaf/seaweed reinforced polypropylene composite. *Materials Today: Proceedings*, 51, 1372–1375. <https://doi.org/10.1016/J.MATPR.2021.11.411>
- Saengchairat, N., Tran, T., & Chua, C. K. (2017). A review: additive manufacturing for active electronic components. In *Virtual and Physical Prototyping* (Vol. 12, Issue 1). <https://doi.org/10.1080/17452759.2016.1253181>
- Shahrubudin, N., Koshy, P., Alipal, J., Kadir, M. H. A., & Lee, T. C. (2020). Challenges of 3D printing technology for manufacturing biomedical products: A case study of

- Malaysian manufacturing firms. *Heliyon*, 6(4).
<https://doi.org/10.1016/j.heliyon.2020.e03734>
- Shahrudin, N., Lee, T. C., & Ramlan, R. (2019). An overview on 3D printing technology: Technological, materials, and applications. *Procedia Manufacturing*, 35.
<https://doi.org/10.1016/j.promfg.2019.06.089>
- Shaik, Y. P., Schuster, J., & Shaik, A. (2021). A Scientific Review on Various Pellet Extruders Used in 3D Printing FDM Processes. *OALib*, 08(08).
<https://doi.org/10.4236/oalib.1107698>
- Shubhra, Q. T. H., Alam, A. K. M. M., & Quaiyyum, M. A. (2013). Mechanical properties of polypropylene composites: A review. In *Journal of Thermoplastic Composite Materials* (Vol. 26, Issue 3). <https://doi.org/10.1177/0892705711428659>
- Silbernagel, C. (2018). *Additive Manufacturing 101-4: What is material jetting?* Canada Makers.
- Tiwari, S. K., Pande, S., Agrawal, S., & Bobade, S. M. (2015). Selection of selective laser sintering materials for different applications. *Rapid Prototyping Journal*, 21(6).
<https://doi.org/10.1108/RPJ-03-2013-0027>
- Tofail, S. A. M., Koumoulos, E. P., Bandyopadhyay, A., Bose, S., O'Donoghue, L., & Charitidis, C. (2018). Additive manufacturing: scientific and technological challenges, market uptake and opportunities. In *Materials Today* (Vol. 21, Issue 1).
<https://doi.org/10.1016/j.mattod.2017.07.001>
- Wang, Y., Blache, R., & Xu, X. (2017). Selection of additive manufacturing processes. *Rapid Prototyping Journal*, 23(2). <https://doi.org/10.1108/RPJ-09-2015-0123>
- Yap, Y. L., Tan, Y. S. E., Tan, H. K. J., Peh, Z. K., Low, X. Y., Yeong, W. Y., Tan, C. S. H., & Laude, A. (2017). 3D printed bio-models for medical applications. *Rapid Prototyping Journal*, 23(2). <https://doi.org/10.1108/RPJ-08-2015-0102>
- Zakaria Razak, Abu Bakar Sulong, Norhamidi Muhamad, Che Hassan Che Haron, Mohd Khairul Fadzly Md Radzi, Dulina Tholibon, Izdihar Tharazi, & Nur Farhani Ismail. (2018). *The effects of maleic anhydride grafted PP (MAPP) on the mechanical properties of injection moulded kenaf/CNTs/PP composites.*
http://www.ukm.my/jsm/english_journals/vol47num6_2018/contentsVol47num6_2018.html
- Zhou, H., Li, W., Hao, X., Zong, G., Yi, X., Xu, J., Ou, R., & Wang, Q. (2022). Recycling end-of-life WPC products into ultra-high-filled, high-performance wood fiber/polyethylene composites: a sustainable strategy for clean and cyclic processing in the WPC industry. *Journal of Materials Research and Technology*, 18, 1–14.
<https://doi.org/10.1016/J.JMRT.2022.02.091>

APPENDICES

APPENDIX A Gantt Chart for PSM1

NO.	TASK PROJECT	WEEK													
		1	2	3	4	5	6	7	8	9	10	11	12	13	14
1.	PSM Briefing	Actual													
2.	Overview Project Background	Actual													
3.	Problem Statement Identification	Actual	Actual	Actual			M								
4.	Define Objective and scope	Actual	Actual	Actual			I								
5.	Literature Studies				Actual	Actual	D								
6.	Methodology						T	Actual	Actual	Actual					
7.	Preliminary Study						E				Actual	Actual	Actual		
8.	Preparation for Presentation						R							Actual	
9.	Report Final Improvement						M							Actual	
10.	Report PSM1 Submission						B							Actual	
11.	Slide Presentation						R							Actual	
							E							Actual	
							A							Actual	
							K							Actual	
														Actual	
														Actual	

Plan
 Actual

APPENDIX B Gantt Chart for PSM2

NO.	TASK PROJECT	WEEK													
		1	2	3	4	5	6	7	8	9	10	11	12	13	14
1.	MEETING AND DISCUSSION														
2.	PREPARATION OF RAW MATERIAL														
3.	CONDUCTING THE EXPERIMENT						M								
4.	COLLECT DATA AND MAKE ANALYSIS ON SAMPLE						I								
5.	DISCUSS ON RESULT EXPERIMENT						D								
6.	START DRAFT REPORT AND WRITING UP CHAPTER 4						T								
7.	START DRAFT REPORT AND WRITING UP CHAPTER 5						E								
8.	SUBMISSION OF FIRST DRAFT PSM 2						R								
9.	RECHECK FIRST DRAFT						M								
10.	WRITING UP CONCLUSION FOR THIS STUDY						B								
11.	SUBMISSION OF FULL REPORT						R								
12.	FINALIZE THE CORRECTION OF FULL REPORT						E								
13.	PREPARATION AND PRESENTATION OF PSM 2						A								
							K								



Plan



Actual

PSM 2 Husaini

PAGE 1

PAGE 2

PAGE 3

PAGE 4

PAGE 5

PAGE 6

PAGE 7

PAGE 8

PAGE 9

PAGE 10

PAGE 11

PAGE 12

PAGE 13

PAGE 14

PAGE 15

PAGE 16

PAGE 17

PAGE 18

PAGE 19

PAGE 20

PAGE 21

PAGE 22

PAGE 23

PAGE 24

PAGE 25



PAGE 26

PAGE 27

PAGE 28

PAGE 29

PAGE 30

PAGE 31

PAGE 32

PAGE 33

PAGE 34

PAGE 35

PAGE 36

PAGE 37

PAGE 38

PAGE 39

PAGE 40

PAGE 41

PAGE 42

PAGE 43

PAGE 44

PAGE 45

PAGE 46

PAGE 47

PAGE 48

PAGE 49

PAGE 50

PAGE 51



PAGE 52

PAGE 53

PAGE 54

PAGE 55

PAGE 56

PAGE 57

PAGE 58

PAGE 59

PAGE 60

PAGE 61

PAGE 62

PAGE 63

PAGE 64

PAGE 65

PAGE 66

PAGE 67

PAGE 68

PAGE 69

PAGE 70

PAGE 71

PAGE 72

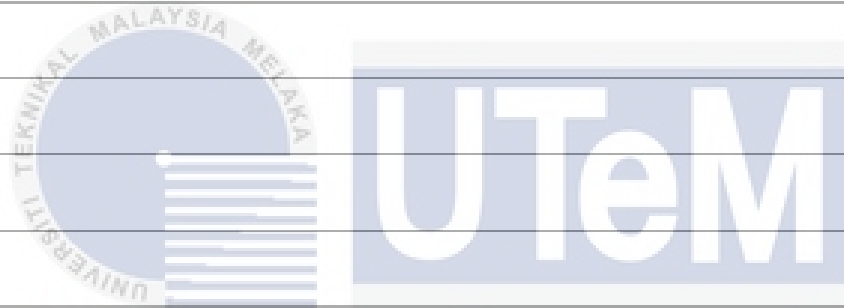
PAGE 73

PAGE 74

PAGE 75

PAGE 76

PAGE 77



اونيورسيتي تيكنيكل مليسيا ملاك

UNIVERSITI TEKNIKAL MALAYSIA MELAKA

PAGE 78

PAGE 79

PAGE 80

PAGE 81

PAGE 82

PAGE 83

PAGE 84

PAGE 85

PAGE 86

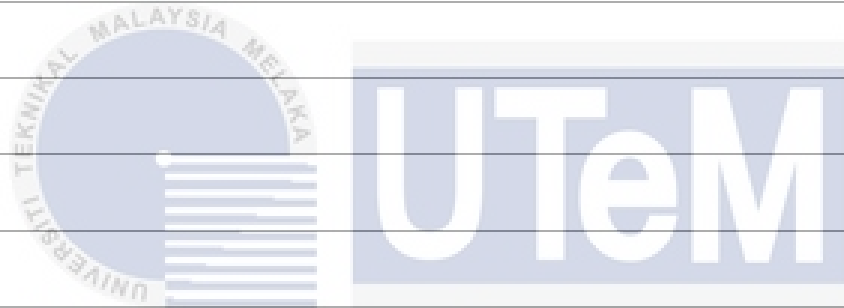
PAGE 87

PAGE 88

PAGE 89

PAGE 90

PAGE 91



اونيورسيتي تيكنيكل مليسيا ملاك

UNIVERSITI TEKNIKAL MALAYSIA MELAKA